AKARI
Observer's Manual for the Post-Helium (Phase 3) Mission

Version 1.2

— for Open Time Observation Planning —

AKARI User Support Team
in

Institute of Space and Astronautical Science / JAXA
contact: iris_help@ir.isas.jaxa.jp
European Space Astronomy Centre / ESA
contact: http://akari.esac.esa.int/esupport/

May 22, 2009

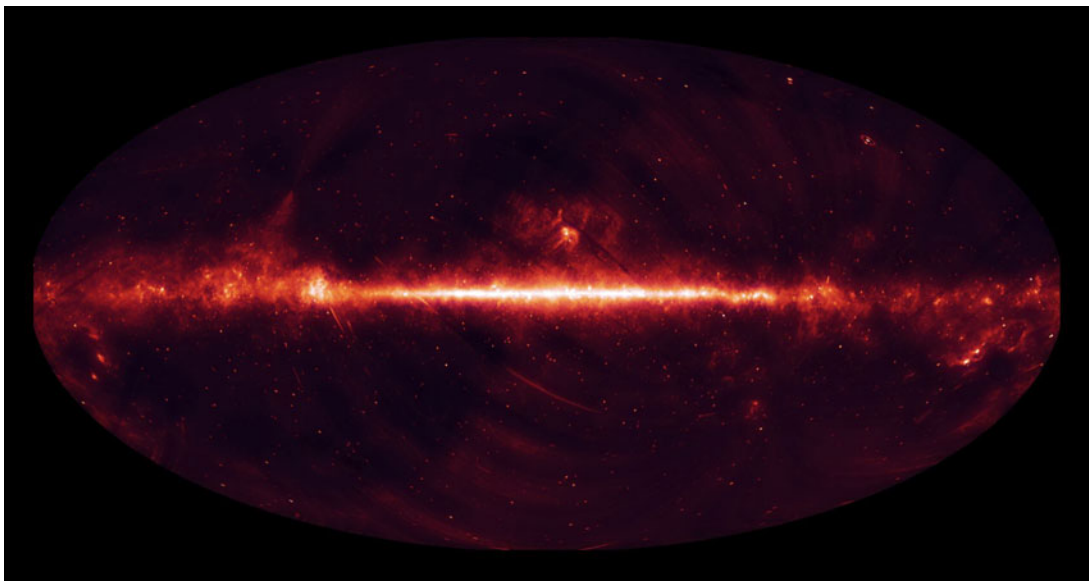

Revision Record

2008 May 12	Version 1.0 released, adapted from ASTRO-F Observer's Manual Version 3.2,
2008 June 12	Version 1.1 released. Cookbook section added in Appendix.
2009 May 8	Version 1.2. Small revisions to update the performance.

Contents

1 Introduction **1**
- 1.1 Purpose of this document . . . 1
- 1.2 Relevant Information . . . 3

2 Mission Overview **5**
- 2.1 The *AKARI* Mission . . . 5
- 2.2 Satellite . . . 6
  - 2.2.1 The Bus Module . . . 6
  - 2.2.2 Attitude Determination and Control System . . . 7
  - 2.2.3 Cryogenics . . . 8
- 2.3 Telescope . . . 9
  - 2.3.1 Specification . . . 9
  - 2.3.2 Capability and Performance in Phase 3 . . . 10
- 2.4 Focal-Plane Instruments . . . 11
  - 2.4.1 Specification Overview . . . 11
  - 2.4.2 Focal-Plane Layout . . . 13
  - 2.4.3 The Focal-Plane Star Sensor (FSTS) . . . 14
- 2.5 The *AKARI* Observation Programms in Phase 3 . . . 15
- 2.6 References . . . 16

3 Satellite Operations **17**
- 3.1 Orbit and Observing Attitude . . . 17
- 3.2 Attitude Operation Modes for Observations . . . 19
  - 3.2.1 Survey Mode . . . 19
  - 3.2.2 Pointing Mode . . . 19
- 3.3 Mission Phases . . . 22
- 3.4 Sky Visibility . . . 23

4 IRC: Infrared Camera **25**
- 4.1 Hardware Specification . . . 26
  - 4.1.1 Overview . . . 26
  - 4.1.2 Optics . . . 27
  - 4.1.3 Filters and Dispersion Elements . . . 28
  - 4.1.4 Field of View (FoV) . . . 29
  - 4.1.5 Slits for Spectroscopy . . . 29
  - 4.1.6 Detectors . . . 30
- 4.2 Flight performance in phase 3 . . . 31
  - 4.2.1 Optics . . . 31
  - 4.2.2 Detector system . . . 35
- 4.3 The IRC Instrument Operation . . . 36

4.3.1 Pointed Observations . . . 36
4.4 The IRC AOTs . . . 38
4.4.1 Detection Limits and Saturation Limits: General Remarks . . . 39
4.4.2 IRCZ0: Deep Imaging Mode . . . 40
4.4.3 Expected Performance . . . 41
4.4.4 IRCZ2: Imaging and Spectroscopy with Two Filters or Filter and Prism . 42
4.4.5 Expected Performance . . . 43
4.4.6 IRCZ3: Imaging with Three Filters . . . 44
4.4.7 Expected Performance . . . 45
4.4.8 IRCZ4: Spectroscopic mode . . . 46
4.4.9 Expected Performance . . . 48
4.5 Notes and Restrictions for the IRC Observations . . . 50

5 Data Reduction and Products 51
5.1 Basic Policy . . . 52
5.1.1 IRC Data Reduction: AOT IRCZ0, Z2, Z3 . . . 52
5.1.2 IRC Data Reduction: AOT IRCZ4 . . . 52
5.1.3 Phase 3 data . . . 52

A AKARI Cookbook for Post-Helium (Phase 3) mission Open Time observations 53
A.1 Introduction . . . 53
A.2 Example 1: Spectroscopy of distant galaxies with the NG grism in the point source aperture . . . 54
A.2.1 Scientific Background . . . 54
A.2.2 Selection of Targets and Target Visibility . . . 55
A.2.3 The Choice of Observation Mode . . . 57
A.2.4 Preparation of Target List . . . 58
A.2.5 Target List Validation . . . 60
A.2.6 Duplication Check . . . 61
A.2.7 Submission of Proposal . . . 62
A.3 Example 2: Spectroscopy of Planetary Nebulae with the IRC . . . 63
A.3.1 Scientific Background . . . 63
A.3.2 Target Visibility . . . 63
A.3.3 The Choice of Observation Mode . . . 65
A.3.4 Preparation of Target List . . . 66
A.3.5 Target List Validation . . . 68
A.3.6 Duplication Checker . . . 68
A.3.7 Submission of Proposal . . . 68
A.4 Example 3: Near-infrared imaging of extragalactic fields with the IRC . . . 70
A.4.1 Scientific Background . . . 70
A.4.2 Selection of Target Field and Target Visibility . . . 71
A.4.3 The Choice of Observation Mode . . . 71
A.4.4 Preparation of Target List . . . 72
A.4.5 Target List Validation . . . 73
A.4.6 Duplication Check Tool . . . 74
A.4.7 Submission of Proposal . . . 76

Chapter 1

Introduction

1.1 Purpose of this document

This *AKARI Observer's Manual*, is issued as the reference for *AKARI* observers, for observation planning and the preparation for the data analysis for the post-Helium mission (hereafter called phase 3).

The document covers the specifications of the satellite and the instruments, their performance, flight operation plan, including definitions of the Astronomical Observation Templates (AOTs), and a brief desscription on the scope of data analysis. It contains the most up-to-date estimates of the detection limits of the instrument based on the phase 3 performance evaluation observations carried out in early 2008.

Note that some of the instrumental performance information was not yet available by the time of the publication of this version of the manual. Frequent updates will be given on the Observer's support Web page.

Figure 1.1.1: *AKARI* (ASTRO-F) waiting for the launch (January, 2006).

1.2 Relevant Information

***AKARI* Observer's Web**

The AKARI Observers Web pages contains some additional information and data useful for the observers, including links to the user support tools:
http://www.ir.isas.jaxa.jp/AKARI/Observation/ for Japanese & Korean Open Time users
http://akari.esac.esa.int/ for the ESA Call: for ESA Open Time Users

Helpdesk

Any questions and comments on *AKARI* observations and user support shall be addressed to the *AKARI* Helpdesks.
iris_help@ir.isas.jaxa.jp: for Japanese & Korean Open Time Users
http://akari.esac.esa.int/esupport/ : for ESA Open Time Users

Chapter 2

Mission Overview

2.1 The *AKARI* Mission

AKARI (previously known as ASTRO-F) is the second Japanese space mission for infrared astronomy. It was launched on February 21, 2006 (UT) by JAXA's M-V rocket. The orbit is a Sun-synchronous polar orbit with an altitude of 700 km and a period of 100 minutes. A pair of Stirling cycle mechanical coolers enabled a long cryogenic mission lifetime with only 170 litres of liquid Helium. The liquid Helium boiled off on August 26, 2007. After the liquid Helium exhaustion the telescope system is kept at about 40 K by the mechanical cooler and observations at near-infrared wavelengths are continued.

AKARI is equipped with a 68.5 cm cooled telescope and two scientific instruments, namely the Far-Infrared Surveyor (FIS) and the Infrared Camera (IRC). The FIS has two 2-dimensional detector arrays and observes in four far-infrared bands between 50 and 180 μm at cryogenic temperatures. The IRC consists of three cameras covering 1.8–26 μm in 9 bands with fields of view of approximately $10' \times 10'$. Both instruments have low- to moderate-resolution spectroscopic capability. Only the near-infrared channel (1.8–5.5 μm) is available for phase 3 observations.

A major goal of the mission is to carry out an All-Sky Survey with the FIS and additionally with the IRC at 9 and 18 μm. The *AKARI* All-Sky Survey will significantly surpass the previous all-sky survey in the infrared by IRAS in both spatial resolution and wavelength coverage. The results will be published as *AKARI* infrared source catalogues. In addition to the survey observations, *AKARI* allowed for dedicated pointed observations with both the FIS and IRC.

Five thousand pointed observations were performed in the cryogenic phase of the mission. Many pointed observations are used for the legacy observations by the *AKARI* project team members. Such programmes are referred to as "Mission Programmes". In addition, 30 percent of pointed observation opportunities were open for general users in Phase 2 in Japan/Korea and ESA related countries via parallel peer-reviewed Call for Proposals.

Many international collaborations are ongoing with the *AKARI* project. The European Space Agency (ESA) supplied a ground station operated by ESOC, and ESAC carries out the pointing reconstruction of the All-Sky Survey observations. ESAC also handles the user support for the European Open Time observing programmes. A consortium of Imperial College University of London, the Open University, University of Sussex, and SRON-Groningen with University of Groningen (IKSG consortium) participates on the data reduction of the FIS All-Sky Survey. Seoul National University representing the Korean community also joins the data reduction activity. Several collaborations at the personal level are also ongoing especially on the celestial calibrators.

2.2 Satellite

Figure 2.2.1 shows the overall structure of the *AKARI* spacecraft. The height is about 3.7 m (excluding the aperture lid) and the launch weight mass 952 kg. The satellite consists of two parts, the bus module and the cryostat. The two parts are connected by a truss structure.

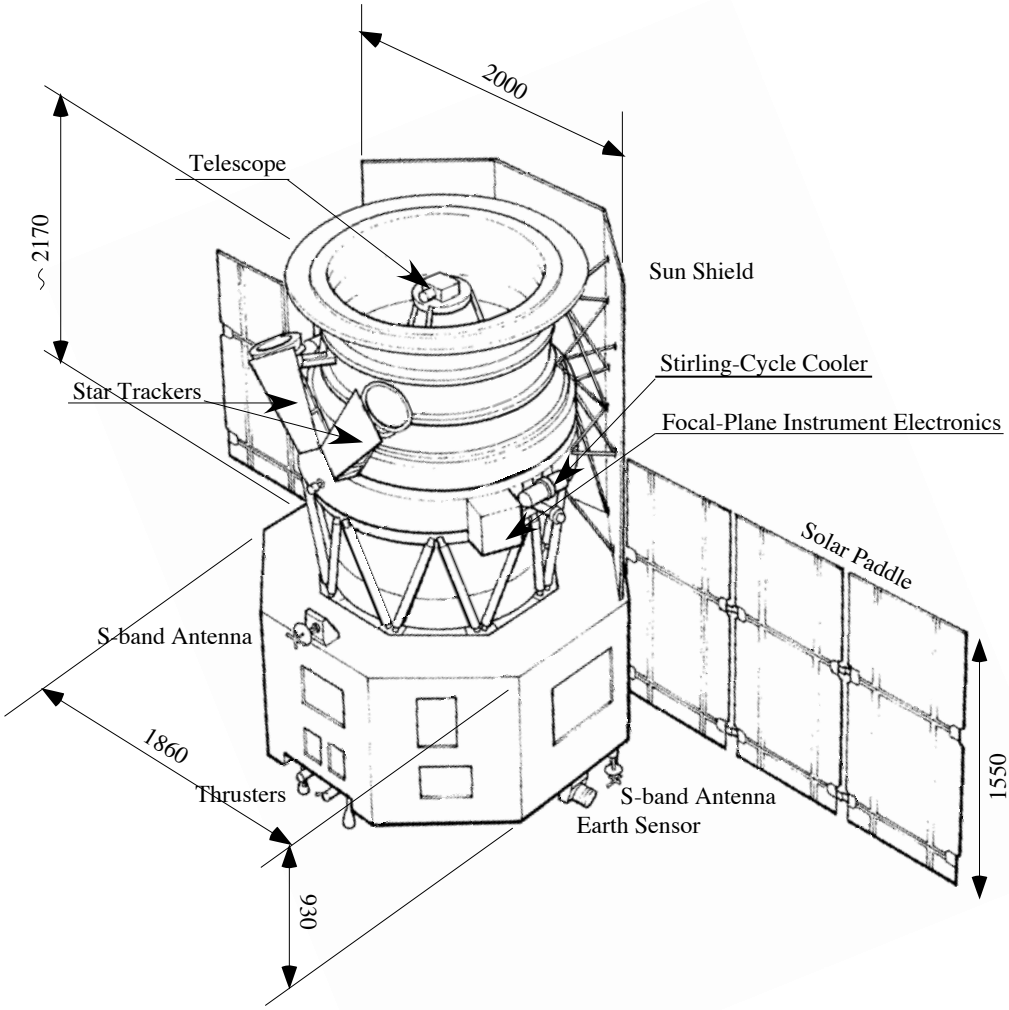

Figure 2.2.1: An overall view of the *AKARI* spacecraft (scales are in mm).

2.2.1 The Bus Module

The bus module takes care of the power supply, house keeping, spacecraft attitude control, data acquisition and the telecommunication link to the ground station. *AKARI* uses the S-band (mainly for command and house-keeping telemetry data) and the X-band (mainly for scientific data) for telecommunication. Due to its' near-Earth orbit, communication between the satellite and the ground stations is limited. Therefore, *AKARI* has a two-Gigabyte data recorder.

2.2.2 Attitude Determination and Control System

The attitude of the *AKARI* satellite is determined and controlled by on-board sensors and a computer unit. Figure 2.2.2 shows the block diagram of the attitude and orbit control system (AOCS). The framework of the system is as follows: The IRU (Gyro) measures the motion of the satellite. The TFSS (Two-dimensional Fine Sun Sensor) were meant to monitor the position of the Sun in two-dimensions perpendicular to the Sun-satellite direction, and to correct any long-term drift of the IRU signal. A pair of Star Sensors (STT) mounted on the wall of the cryostat are used to observe the attitude along the third axis and the alignment change between the bus module, where IRU and TFSS are located, and the cryostat in which the telescope is installed. Other instruments provide additional information for attitude determination. A dedicated computer (AOCU) determines the satellite attitude. A set of reaction wheels (RW) control the spacecraft attitude, with the help of Magnetic Torque Rods (MTQ). In the case of any very large required motion, a set of thrusters may be used.

In the initial phase of the mission, the TFSS were found not to detect the Sun properly. This was overcome with a new version of the on-board software for the attitude and orbit control subsystem, making use of the Star Trackers.

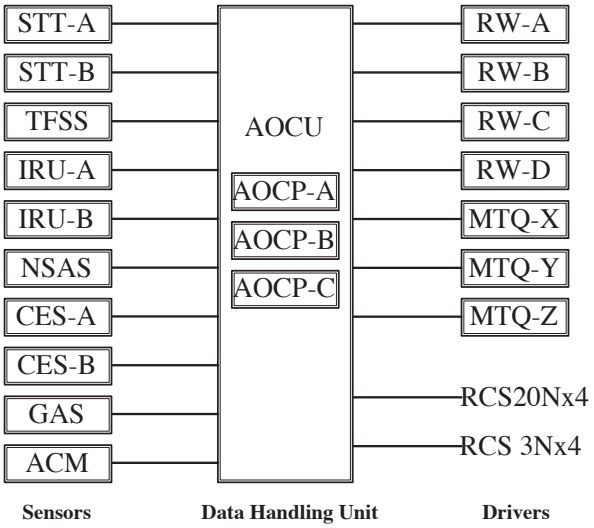

Figure 2.2.2: Block diagram of the *AKARI* attitude determination and control system.

2.2.3 Cryogenics

Scientific instruments are all stored in the cryostat and were maintained at cryogenic temperatures by 170 litres of super-fluid liquid Helium with the help of two sets of Stirling-cycle coolers. The near-infrared instrument is operated with the mechanical coolers after the liquid Helium boil-off. *AKARI* is operated with the Sun-shield always directed to the Sun. The cryostat is covered by silver coated film that reflects visible light but radiates in the infrared.

The Scientific Instrument Assembly (SIA), namely the telescope and the Focal-Plane Instruments (FPI) are thermally shielded by two layers of Vapour Cooled Shield (VCS) in which Helium vapour evaporated from the tank was running through. The inner VSC is also cooled by the mechanical coolers. The SIA was mainly cooled by the Helium vapour down to about 6 K. The FIS body and two detectors are directly connected to the Helium tank via thermal straps and were operated at 2.0–2.2 K. After the liquid Helium boiled-off, the SIA is kept around 40 K and near-infrared observations are being carried out.

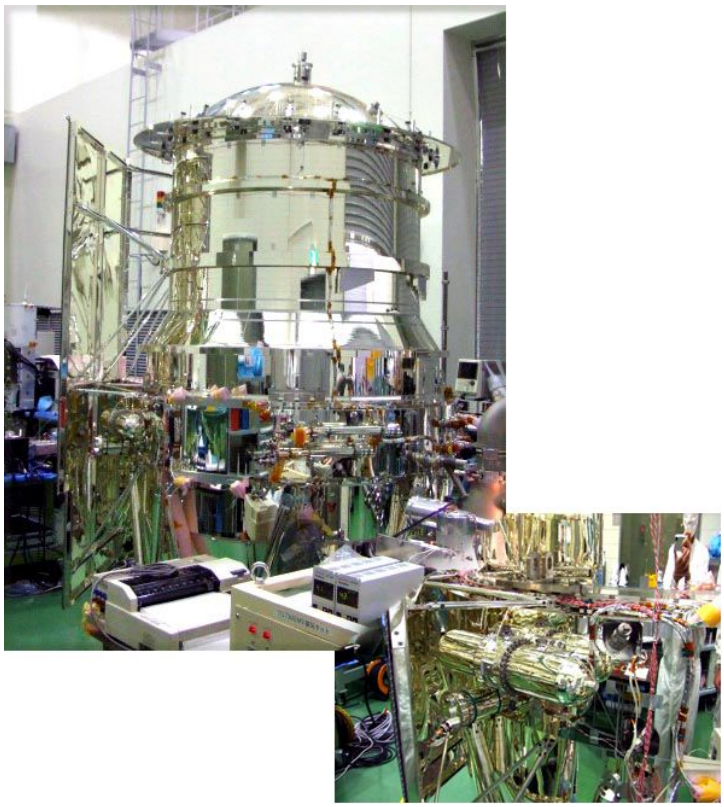

Figure 2.2.3: The *AKARI* Cryogenic system in the clean room for maintenance. (Left) The Cryostat. (Right) Close-up of the Two-Stage Stirling cooler. (Photo: July, 2005)

2.3 Telescope

2.3.1 Specification

The telescope is a Rithcy-Chrétien system with an effective aperture of 68.5 cm and a focal ratio of 6.1 (Figure 2.3.4). The mirrors are made of SiC porous+CVD coated material. This rigid material allowed to reduce the weight of the mirrors significantly. The primary mirror, with a physical diameter of 71 cm, weighs only 11 kg. The total weight of the telescope system is 42 kg. The focus may be adjusted in orbit during the PV phase by moving the position of the secondary mirror. The parameters for the telescope are summarized in Table 2.3.1.

The primary mirror was replaced in 2004 as a part of a refurbishment of the telescope system. The effective aperture has been increased slightly (previously 67 cm). The telescope has been tested in the cryogenic vibration tests, and the mirror support system which previously had a problem has been confirmed to be secure.

Figure 2.3.4: The *AKARI* telescope system.

Table 2.3.1: Telescope Specification

Effective diameter	68.5 cm (primary mirror)
Focal length	420 cm
Focal ratio	6.1
Optical design	Ritchey-Chrétien type

2.3.2 Capability and Performance in Phase 3

Mirror surface accuracy has been measured at cryogenic temperatures to be as low as 9 K. Due to thermal stress at the supporting points, the wave front error becomes larger at low temperatures and is at its' worst at around 50 K.

The in-orbit performance of the *AKARI* telescope system was measured to be diffraction limited at a wavelength of 7.3 μm at 6 K. The image quality in phase 3 has been estimated to be by about 10% degraded from that at 6 K after the focus adjustment.

During the Helium period, the stray light scattered off the top of the baffle was noticed particularly during the periods around solstices. This stray light is expected to persist in phase 3 and observations of diffuse emission need to be arranged carefully.

AKARI phase 3 observations provide a unique capability in broad band imaging with a large FoV ($10' \times 9.3'$) as well as low-resolution spectroscopy in 2–5 μm. In particular, the spectroscopic mode provides slit-less spectroscopy for the first time in space missions. It enables efficient multi-object spectroscopy in one pointing observation. High-sensitivity near-infrared spectroscopy free from disturbance of the terrestrial atmosphere can be applied for studies in various astronomical objects.

2.4 Focal-Plane Instruments

2.4.1 Specification Overview

Two scientific instruments are placed in the Focal-Plane of the telescope; the Far-Infrared Surveyor (FIS) and the Infrared Camera (IRC). In addition, two sets of Focal-Plane Star Sensors (FSTS) are installed for observing guide stars in the Near Infrared band ($\sim$ J-band) for pointing reconstruction during the survey observations. **In phase 3, only the near-infrared channel of the IRC is available for observations.** The whole payload capability is reported below for historical reasons.

The FIS is equipped with two sets of two-dimensional detector arrays. The Short-Wavelength channel (SW; 50–110 μm) uses two monolithic Ge:Ga arrays[1] of 20×3 and 20×2 pixels, while the Long-Wavelength channel (LW; 110–180 μm) has a stressed Ge:Ga array of $15 \times 3 + 15 \times 2$ pixels. Each of the four arrays corresponds to a different wavelength band. The pixel sizes are 27 and 44 arcsec^2, respectively.

The IRC consists of three independent cameras; the NIR (2–5 μm), the MIR-S (5–13 μm), and the MIR-L (13–26 μm). The NIR camera has a 512×412 pixel InSb array, of which 100×412 pixels are dedicated for slit spectroscopy. The two MIR cameras use 256×256 pixel Si:As detectors.

The wavelength range and resolving power provided by the scientific instruments are shown in Figure 2.4.5. The spatial resolution and the Field of View (FoV) of the instruments are summarized in Figure 2.4.6.

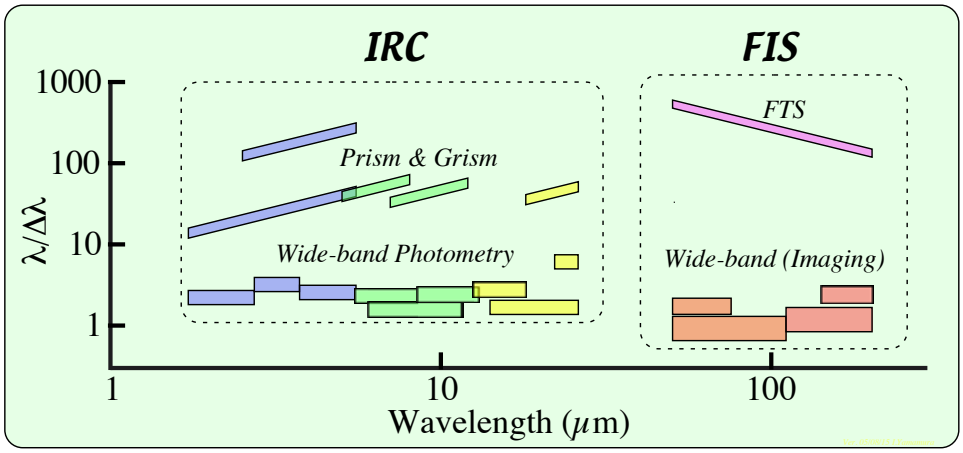

Figure 2.4.5: The wavelength coverage and resolving power of the *AKARI* instruments.

[1]The SW detector was manufactured by NICT.

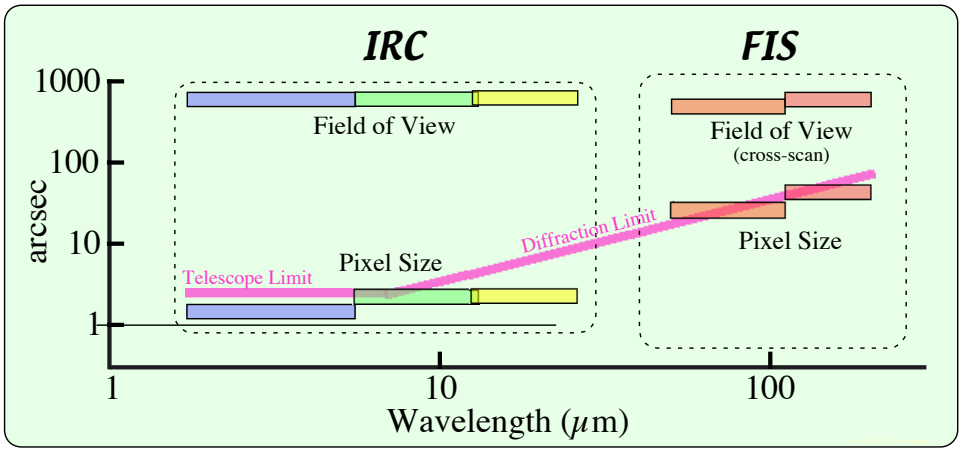

Figure 2.4.6: Pixel size and field of view (FoV) of the *AKARI* on board instruments.

2.4.2 Focal-Plane Layout

Figure 2.4.7 shows the Focal-Plane layout projected onto the sky. There are three light entrances to the instruments; one for the FIS and two for the IRC. The two instruments essentially can observe simultaneously, but they see different areas of the sky as shown in the figure. Therefore, observations of a sky position with different aperture have to be made on different orbits.

The incident infrared radiation coming into the FIS aperture is divided into two spectral domains by a dichroic beam splitter, as a result of which the FIS-SW and LW detector arrays observe almost the same sky position. Similarly, the NIR and MIR-S cameras of the IRC share the same FoV so as to observe the same sky position. Only the MIR-L channel observes a different sky position.

The scan path is approximately parallel to the Ecliptic meridian line. The scan direction depends on the launch configuration, namely the launch time (morning or evening). The actual launch has been in the morning. The FoV is thus moving downward, i.e., stars go through the detector from bottom to top on the figure.

Note that the real position and the shape of each Focal-Plane Instrument on the sky will be slightly different from those shown in Figure 2.4.7, due to optical aberration. See Section 4.1.4 (IRC) for details.

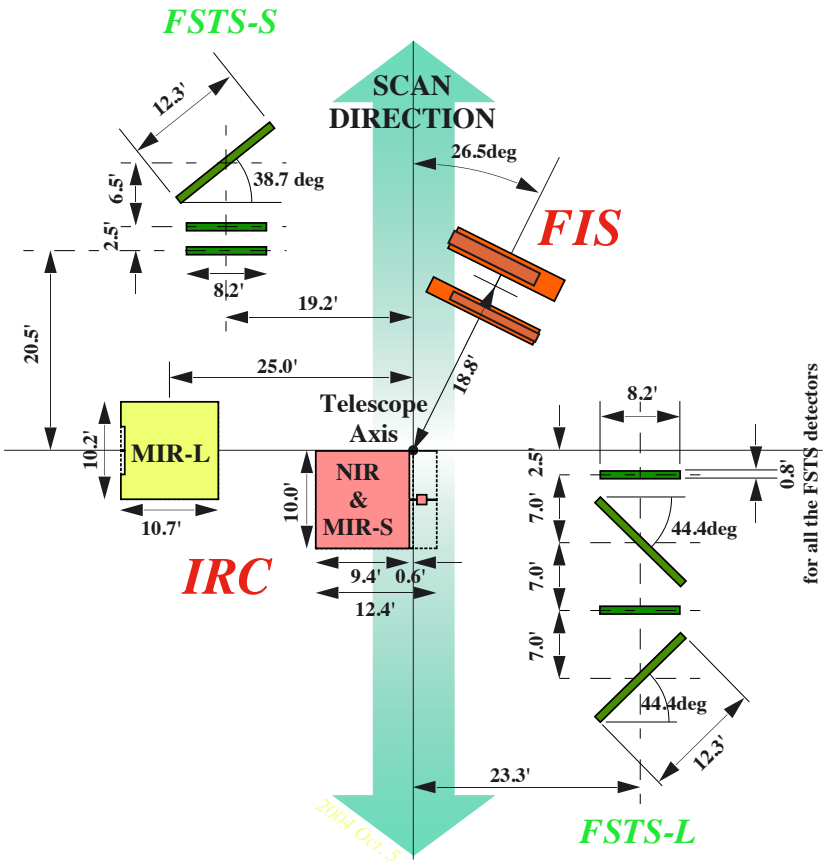

Figure 2.4.7: Focal-Plane layout projected onto the sky. The distortion due to the telescope and instrumental optics have to be taken into account for the data reduction. See the Instrument Data User Manuals for details.

2.4.3 The Focal-Plane Star Sensor (FSTS)

A pair of star sensors are installed in the Focal-Plane. The *FSTS-L* consists of four Ge detector elements[2], while the *FSTS-S* has three. They observe stars with their intrinsic wavelength band profile close to the J-band (1.25 μm). The readout is a TIA (TransImpedance Amplifier) circuit with a sampling rate of about 50 Hz. The seven detectors are sampled almost simultaneously.

As the satellite scans the sky, stars cross the detectors in the in-scan direction one after another. The detection interval between a pair of two horizontal detectors placed in parallel defines the scan speed, and the interval between the tilted and horizontal detectors can be converted to the cross-scan position. The two FSTS's located in opposite corners provide information on the roll angle of the Focal-Plane with respect to the scan direction, as well as a redundancy for the star detection. The absolute positional information is given by comparing the detection information with the position reference catalogue. The pointing reconstruction using the FSTS assumes (all-sky) survey operation mode.

The FSTS is not used in phase 3.

[2]One of the four elements is known to be dead. The effect of this loss to the pointing reconstruction is expected to be small.

2.5 The *AKARI* Observation Programms in Phase 3

Phase 3 Observations with *AKARI* can be divided into the following three categories.

Director and Calibration time (DT): 10 percent of the pointed observation opportunities are reserved for calibration and director's time.

Mission Programmes (MP): 60 percent of the pointed observation opportunities are allocated to the *AKARI* team members as a kind of guaranteed observation time. Specific working groups in every scientific field have worked to establish the observing programmes. In total 16 Mission Programmes are now assigned. The data will be used by the team members for a one year prioritized period and then will be opened to the public. The MP observations are regarded as the legacy of the *AKARI* mission.

Open Time Programmes (OT): 30 per cent of the total pointing opportunities are available to the general research community. Two thirds of the opportunities (= 20 percent of the total) are reserved for Japanese/Korean astronomers, and 10 percent are for the ESA member countries. (see document "Call for Observing Proposals: Policies and Procedures" for more details)

2.6 References

The following papers in the special issue of the Publications of the Astronomical Society of Japan (PASJ) give detailed information on the *AKARI* mission as well as *AKARI* instruments. They describe the in-orbit performance in the cryogenic period and are available at http://pasj.asj.or.jp/v59/v59sp2.html. The performance of phase 3 is described in the present manual as well as on the web.

Mission Overview: The Infrared Astronomical Mission *AKARI*
Murakami, H. et al. 2007, PASJ, 59, S369.

Cryogenics: Flight Performance of the *AKARI* Cryogenic System
Nakagawa, T. et al. 2007, PASJ, 59, S377.

Telescope: In-Orbit Focal Adjustment of the *AKARI* Telescope with Infrared Camera (IRC) Images
Kaneda, H. et al. 2007, PASJ, 59, S411.

FIS: The Far-Infrared Surveyor (FIS) for *AKARI*
Kawada, M. et al. 2007, PASJ, 59, S389.

IRC: The Infrared Camera (IRC) for *AKARI* – Design and Imaging Performance
Onaka, T. et al. 2007, PASJ, 59, S401.

IRC spectroscopy: Near-Infrared and Mid-Infrared Spectroscopy with the Infrared Camera (IRC) for *AKARI*
Ohyama, Y. et al. 2007, PASJ, 49, S411.

Chapter 3

Satellite Operations

3.1 Orbit and Observing Attitude

The orbit of *AKARI* is a Sun-synchronous polar orbit along the twilight zone with an altitude of 700 km, corresponding to an orbital period of 100 min. After the liquid Helium boil-off, the orbit was readjusted to a nearly ideal Sun-synchronous polar orbit.

In principle, the spacecraft always points in the direction perpendicular to the Sun–Earth line, keeping the Sun-shield towards the Sun, and rotates once per orbit to look out in the opposite direction to the Earth. The spacecraft attitude in the cross-scan direction[1] has a flexibility of ± 1 degree about the canonical scan path.

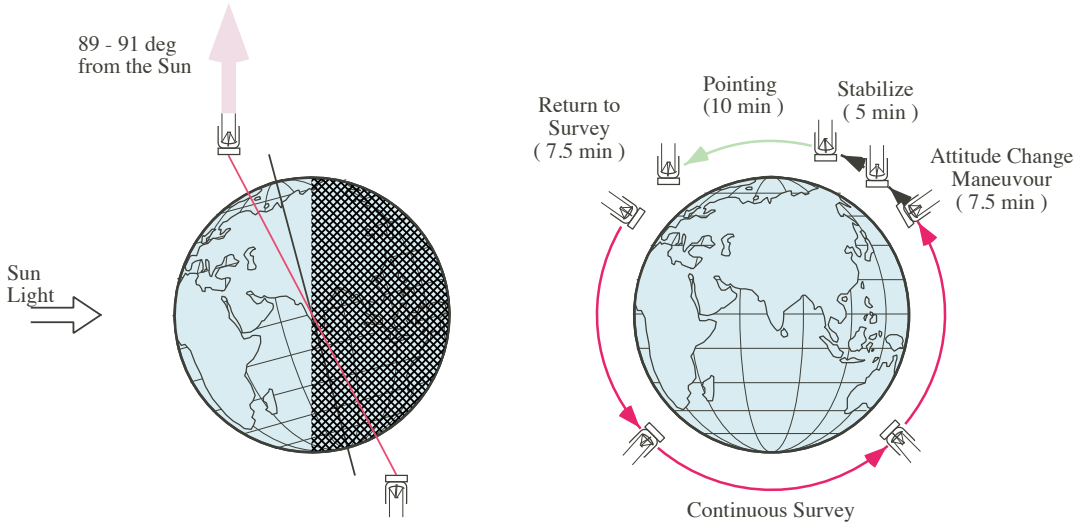

Figure 3.1.1: The in-orbit attitude of *AKARI* (left) and the pointed observation maneuver (right).

In the survey mode, the satellite is operated such that the telescope scans the sky with a constant speed (3.6 arcmin / sec) usually along the great-circle at a solar-elongation of 90 degrees. In the pointing mode, the telescope can point at an area of the sky along the scan path for up to 10 minutes, with the total cost of 30 minutes including maneuver for the operation. Observations in phase 3 will be carried out only in pointing mode. The survey mode satellite operations will however still be conducted as designed. Fine control of the observing position

[1] the direction perpendicular to the scanning (in-scan) direction.

in a pointing operation is possible. Observations in the pointing mode are defined by a set of Astronomical Observation Templates (AOT; see Sections 4.4).

The satellite Attitude and Orbit Control System (AOCS) has the capability of determining / controlling the absolute attitude to an accuracy of 30 arcsec. The dominant source of the pointing uncertainty is the alignment of the focal-plane axis with respect to the AOCS reference frame on the bus module and its time variation due to thermal distortion of the spacecraft.

Table 3.1.1 summarizes the nominal operation parameters and expected performance of the *AKARI* AOCS for astronomical observations.

Table 3.1.1: *AKARI* AOCS Specifications

Absolute Pointing Control Accuracy	30 arcsec
Scan Speed Stability (in-scan)	< 0.1 per cent
Scan Speed Stability (cross-scan)	3×10^{-5} arcsec/min
Pointing Stability	< 1 arcsec/min (peak-to-peak)

3.2 Attitude Operation Modes for Observations

3.2.1 Survey Mode

The survey mode is not used in observations of phase 3. This section is left over for information.

In the survey mode, *AKARI* performs a continuous scan of the sky. The spacecraft spins around the Sun-pointed axis once every orbit, keeping the telescope pointed toward the opposite direction to the Earth (see left-hand of Figure 3.1.1); as a result, the telescope traces a great circle with a solar elongation of 90 deg. The orbital period of 100 minutes corresponds to a scan-speed of 3.6 arcmin s^{-1}. In Table 3.2.2, the specification and performance of the survey mode operation are summarized.

Table 3.2.2: Summary of Survey mode operation (nominal).

Specification of Survey mode operation	
Survey Scan Speed	3.6 arcmin s^{-1}
Survey In-scan Stability[1]	≤ 0.1 per cent
Survey Cross-scan Stability[1]	$\sim 3 \times 10^{-5}$ deg/sec (3σ)
Pointing determination error (goal)	
On-board	< 30 arcsec (in-scan and cross-scan)
G-ADS	15–30 arcsec (in-scan and cross-scan)
Pointing Reconstruction (During Mission)	< 5 arcsec (in-scan), < 7 arcsec (cross-scan)
Pointing Reconstruction (Post-Mission)	< 3 arcsec (in-scan), < 5 arcsec (cross-scan)

[1] Based on the performance evaluation tests.

The accurate position of the survey scan path on the sky is determined during the pointing reconstruction processing. There are three levels of the processing: on-board determination by the attitude and orbit control system (AOCS), on-ground processing using the same dataset (G-ADS), and detailed analysis together with the Focal-Plane Star Sensor (FSTS) and IRC survey data.

The outline of the attitude determination process is summarized in Figure 3.2.2. The on-board attitude analysis has an absolute error of $\sim$ 30 arcsec. The main source of this error is the alignment uncertainty between the satellite AOCS and the telescope's focal-plane. The results of the on-board analysis are downloaded to the ground with the sensor signal data. The data is re-analyzed by the G-ADS for cross-check and to prepare the initial pointing data for reconstruction. At this stage, the pointing data (in the survey mode) still has an error of 15–30 arcsec.

Then, the data from the FSTS and the IRC survey are analyzed together with the initial pointing data for refinement (pointing reconstruction). The ESA European Space Astronomy Centre (ESAC) is in charge of the final pointing reconstruction. The goal of the pointing accuracy after the reconstruction is 5 arcsec (in-scan) and 7 arcsec (cross-scan) during the survey. This accuracy can be improved to 3 arcsec (in-scan) and 5 arcsec (cross-scan) when the survey is completed and all data are analyzed and reprocessed.

3.2.2 Pointing Mode

In the pointing mode, *AKARI* will observe a specific sky position. Both imaging and spectroscopic observations with longer exposure times than the survey are possible. A single pointed observation consists of four continuous operations (Figure 3.1.1, right);

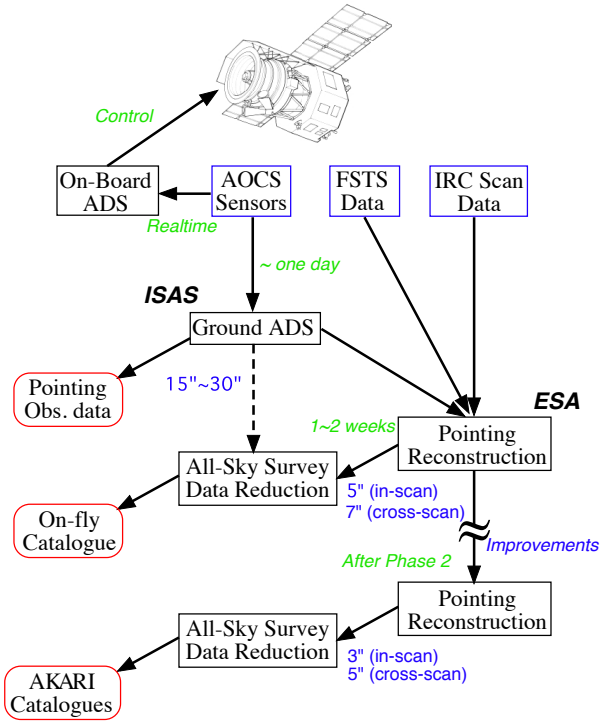

Figure 3.2.2: The outline of the *AKARI* attitude determination for the All-Sky Survey, including time scales and envisioned accuracy improvement. Note that the pointing reconstruction by ESA is not carried out for the pointed observations.

1. Slewing maneuver to point the telescope at the target position,
2. Stabilization of the telescope,
3. Observation of the target,
4. Returning to the survey mode.

The total operation is completed in 30 minutes. This means that the maximum number of pointed observations per orbit is three, if and when we can find a suitable set of targets separated by $\sim$ 120 deg. The actual net observation time per pointing is however limited to 10 minutes. To increase the flexibility of the observation opportunity for any target, the telescope can point at any position on the sky in a stripe of 2 degree ($\pm$1 deg) perpendicular to the nominal scan path. However, this allowance is much smaller than previous missions such as IRAS, ISO and Spitzer. Observers have to understand that the visibility of *AKARI* to observe a specific target is extremely limited.

In order to avoid the Earth-light, the satellite starts slewing back to the survey mode automatically if the avoidance angle exceeds the limit. This happens without notifying the instruments to complete the observation. As a result, the very last part of some observation data may be lost in some unfortunate cases. In Table 3.2.3, we summarize the specifications of the pointing mode.

The FoV is allowed to shift by a small amount in a pointed observation in the way summarized in Table 3.2.4.

These fine control operations are all included in the AOTs, and users do not have to concern themselves with them. An IRC observation uses Micro-Scan for dithering. See the AOT description page for more details.

The Micro-Scan will cause a disturbance of the satellite attitude at the level of a few arcseconds. Therefore, each exposure has to be started after waiting for the stabilization of the

Table 3.2.3: Summary of Pointing mode operation (nominal)

Specification of Pointing mode operation	
Total operation time	30 min
Maximum observation time	10 min
Absolute accuracy of pointing	30 arcsec
Cross-scan Offset	±1 deg
Performance	
Pointing Stability[1]	$\leq$ 1 arcsec (peak-to-peak) in 1 minutes

[1] Based on the performance evaluation tests.

Table 3.2.4: Pointing adjustment during a Pointed observation.

	Amount of shift	Direction	Purpose
Micro-Scan	15–30 arcsec/step	arbitrary	Dithering of IRC imaging

Use of the Micro-scan is defined in the AOT and observers are not allowed to change it.

telescope attitude. The IRC waits for notification from the AOCS and then starts an exposure. This waiting time will be a dead time for observers. The dead time for Micro-Scan operations is typically about 30 sec and 40–50 sec. It is noted that the actual stabilization time varies depending on the given condition. These dead times are taken into account in the AOTs of the IRC and the corresponding sensitivity estimates.

No pointing reconstruction using the Focal-Plane instruments is planned for the pointed observations. The users will receive position information from the G-ADS. Since the source of the pointing uncertainty is the alignment of the telescope and the AOCS, it is expected that the accuracy will be improved as the analysis progresses. The users can refine the position using the data themselves for the IRC imaging observations.

Due to the trouble encountered at the start of the mission, the TFSS is not used in the attitude control. This leads to an attitude control heavily relying on the Star Trackers, thus imposing additional constraints in the pointed observations. Pointed observations requiring maneuvering in the South Atlantic Anomaly (SAA) are not allowed. In addition, pointed observations in an area where few stars are detectable by the Star Trackers will not be executed.

3.3 Mission Phases

The mission lifetime of *AKARI* is divided into three observation phases excluding the performance verification (PV) phases.

Phase 0 (PV Phase) The first month after the jettison of the aperture lid was assigned to the PV phase. In this period, a check out of the spacecraft system and the Focal-Plane Instruments was made, the in-flight performance was evaluated and the initial calibration of the Focal-Plane Instruments was carried out. Test observations were also performed. This phase lasted from April 13, 2006 to May 8, 2006.

Phase 1 The first half year, during which *AKARI* scanned the entire ecliptic longitude is referred to as Phase 1. In this period, the Large Area Survey Programmes, namely the All-Sky Survey and the NEP / LMC pointing surveys were carried out with highest priority. Some Mission Programme observations were also performed,

Phase 2 This phase continued until 2007 August 26, when all liquid Helium evaporated. Pointed observations of Mission Programmes and Open Time proposals were performed as well as supplemental scan observations to complete the All-Sky Survey.

Phase 3 After the boil-off of the liquid Helium, the mechanical cooler keeps the temperature low enough to observe with the IRC/NIR camera. Phase 3, where only the IRC/NIR camera is operated, continues until any of the on-board instrument (the NIR camera itself, mechanical coolers etc.) cease to function. Performance verification observations for phase 3 had been carried out until phase 3 Mission Programme observations started on June 1, 2008. Open Time programmes for phase 3 started on October 15, 2008.

3.4 Sky Visibility

As noted earlier, the direction of the telescope pointing is always perpendicular to the direction toward the Sun with a flexibility of ±1 deg in the cross-scan direction. Since *AKARI* is in a polar-orbit, the visibility, defined as the number of scan paths covering a particular sky position, is a strong function of ecliptic latitude. Targets in the ecliptic pole regions are observable on a number of orbits, while targets near the ecliptic plane are visible by *AKARI* for only two days (29 orbits) in a half year at most. In addition, visibility is also affected by the SAA (South Atlantic Anomaly; where a large flux of charged particles disturbs the observation when the satellite pass through the region) and the Moon (the moonlight can enter the telescope aperture. The avoidance angle is 33 deg).

Observers should understand that opportunities to observe particular objects or fields with *AKARI* are strictly limited and are a strong function of the ecliptic latitude. It is strongly recommended to the observers to check the visibility at each target position. A Web interface visibility check tool is provided on the Phase 3 observers pages, with which the observers can check the visibility.

[Notes for the Solar System Observation]

Due to the severe visibility constraint, observation planning for Solar System Targets requires additional procedures. The following steps are suggested.

1. Calculate the target position for the corresponding observation dates. This can be done with NASA/JPL's HORIZON system (http://ssd.jpl.nasa.gov/cgi-bin/eph) by giving the condition of solar elongation angle as 90 ± 1 deg.

2. Use the visibility tool following the link from the Phase 3 AO page, to check if the target is really visible at that position at that date.

3. Create the Target List with the coordinates. The corresponding observing date has to be given in the comment field of the Target List.

4. Check the visibility again with the visibility tool.

Chapter 4

IRC: Infrared Camera

The Infrared Camera (IRC) on board *AKARI* is designed to perform deep imaging observations in pointed observing mode. It's unique wide field coverage of 10×10 arcmin^2 is ideal for survey-type observations. The IRC's low-resolution spectroscopic capabilities in the imaging field are also well suited for multi-object spectroscopic surveys. In this section the description of the mid-infrared channels is left over for reference in several places, but only the near-infrared channel is available for phase 3 observations. The performance numbers given in this section were derived from observations in phase 2. Changes from phase 2 observations are indicated. For details of the data processing, please see the IRC Data User Manual.

4.1 Hardware Specification

4.1.1 Overview

The IRC consists of three cameras: NIR, MIR-S and MIR-L, covering the wavelength ranges of 2–5, 5–13, 12–26 μm, respectively. In Table 4.1.1, the specifications of each camera are listed. See also figure 2.4.5 and 2.4.6. Note that only the NIR is available for phase 3 observations.

Table 4.1.1: Specifications of the Infrared Camera (IRC).

Channel	NIR	MIR-S	MIR-L
Detector	InSb(SBRC-189)	Si:As (CRC-744)	Si:As (CRC-744)
Array	512 × 412	256 × 256	256 × 256
Imaging FoV (arcmin^2)[1]	9.3 × 10.0	9.1 × 10.0	10.3 × 10.2
Imaging Area (pixel^2)[1]	391 × 412	233 × 256	246 × 256
Pixel Size (arcsec)	1.46 × 1.46	2.34 × 2.34	2.51 × 2.39
Wavelength (μm)	1.8–5.5	4.6–13.4	12.6–26.5
Filters	N2, N3, N4	S7, S9W, S11	L15, L18W, L24
Dispersion Elements	NP, NG	SG1, SG2	LG2

[1]Cross-scan × in-scan. Masked areas are excluded.

Each camera is equipped with three filters and two dispersion elements. The filter selection is preset in the Astronomical Observation Templates (AOTs; Section 4.4) and cannot be freely chosen by the observers.

4.1.2 Optics

All three cameras of the IRC are off-axis, refractive optical systems. Each camera uses 2–5 lenses. A Ge beam-splitter divides the light between the NIR and MIR-S cameras. Transmitted light comes into the NIR channel. Chromatic aberration does exist in the cameras and is largest in the MIR-S camera which uses only two lenses.

A filter wheel is placed at the iris of each camera. Three filters, two dispersion elements, and a blind mask are prepared for each camera. The blind position is used for dark measurements during the flight operation.

4.1.3 Filters and Dispersion Elements

Table 4.1.2 shows the filters and the dispersion elements of the NIR channel of the IRC.

The NIR camera covers three independent wavelength bands that very roughly correspond to the well known K, L, and M bands. The two dispersion elements of the NIR camera provide different spectral resolutions over a similar wavelength range.

Table 4.1.2: IRC Filters and Dispersion Elements

(1) Channel	(2) Name	(3)	(4) $\lambda_{\rm ref}$ (μ m)	(5) Wavelength (μ m)	(6) $\lambda_{\rm iso}$ (μ m)	(7) $\Delta\lambda$ (μ m)	(8) Dispersion (μ m/pix)
NIR	N2	filter	2.4	1.9–2.8	2.34	0.71	—
	N3	filter	3.2	2.7–3.8	3.19	0.87	—
	N4	filter	4.1	3.6–5.3	4.33	1.53	—
	NP	prism	—	1.8–5.5	—	—	0.06 at 3.5 μm
	NG	grism	—	2.5–5.0	—	—	0.0097

(4) Reference wavelength
(5) Defined as where the responsivity for a given energy is larger than $1/e$ of the peak.
(6) Isophotal wavelength of the filter band for Vega.
(7) Effective bandwidth.
(8) Dispersion power of prism depends on wavelength. The actual resolution can be estimated assuming point spread function (see Table 4.2.4).

4.1.4 Field of View (FoV)

Figure 4.1.1 shows the location of the FoV of the three IRC cameras on the Focal-Plane projected onto the sky (See also Figure 2.4.7). As noted earlier, the NIR and MIR-S cameras observe the same FoV on the sky simultaneously.

Reference positions for the AOT configurations for pointed observations are indicated in blue in Figure 4.1.1. Phase 3 imaging observations (AOT IRCZ0, IRCZ2, and IRCZ3) have a unique reference position, the center position of the NIR camera,'N'. Reference positions for spectroscopic observations (AOT IRCZ4) are explained in the following section.

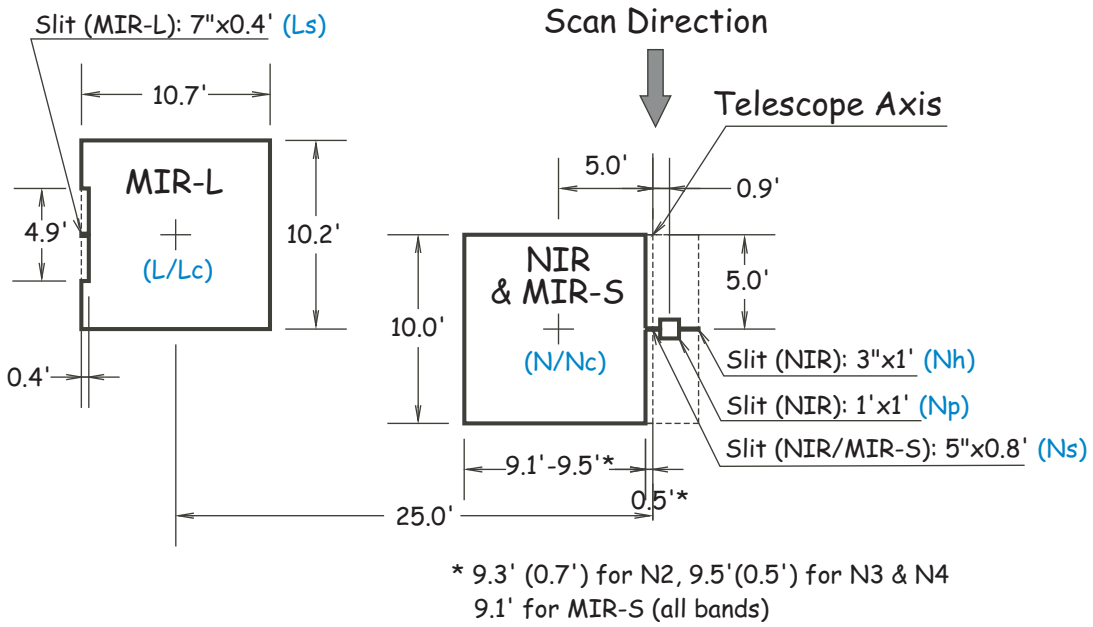

Figure 4.1.1: Focal-Plane layout of the IRC cameras. Reference positions for pointed observations are indicated in blue.

4.1.5 Slits for Spectroscopy

The dispersion elements of the IRC are set into the filter wheel so that all the light in the FoV is dispersed. A spectrum is obtained in the direction parallel to the scan path (in-scan direction), which runs along the vertical direction in Figures 2.4.7 and 4.1.1. Slits are provided for each camera (Figure 4.1.1) in order to avoid contamination by nearby sources / diffuse radiation. The slits are primarily designed for extended sources and it should not be assumed that they can be used to guide a point source into the slit, except for the NIR camera which has an aperture for point sources.

The slit for the NIR camera consists of three parts of different widths. The left most (closest to the imaging area) has a 5 arcsec width and was mainly used for simultaneous observations of diffuse light with the MIR-S camera. This slit position is labeled as 'Ns' for IRCZ4 AOT observation parameter. Both the NP (low-resolution prism) and NG (high-resolution grism) will be used with this slit. The middle $1' \times 1'$ square part, referred to as 'Np' is for spectroscopy of point sources. The aperture is large compared to the absolute pointing accuracy of the satellite (designed to be better than 30 arcsec) to ensure that the target can be accurately guided into the area. Note that for observations of faint sources, confusion due to galaxies may be a serious problem. The NG (grism) is assumed to be used with this aperture. The rightmost (outer)

part ('Nh') has a 3 arcsec width and is used for the highest resolution spectroscopy of diffuse radiation with the NG (grism).

4.1.6 Detectors

The detectors of the IRC are provided by Raytheon IRCoE. The NIR camera has an InSb detector array of 512×412 pixels (SBRC-189), in which 391×412 pixels are used for imaging and the other 121×412 pixels are for slit spectroscopy.

It is known that the detector performance sensitivity changes with temperature. All detector arrays are equipped with thermometers to monitor the module temperature during their operation. In phase 3 it is noticed that the number of hot pixels in the NIR detector is increased drastically from phase 2.

4.2 Flight performance in phase 3

4.2.1 Optics

Field of View (FoV)

The FoV of the NIR is different for different filters depending on the alignment of the filters. A summary is given in Table 4.2.3.

Table 4.2.3: NIR camera FoV sizes

Band	FoV (arcmin^2)
N2	9.3×10.0
N3	9.5×10.0
N4	9.5×10.0

Point Spread Function (PSF)

The performance of the *AKARI* telescope in phase 2 was derived to be diffraction limited at $\sim$ 7.3 μm and it was confirmed that the image quality was degraded by 10–20% in phase 3. Thus the PSF is more extended than the diffraction limits in the NIR camera. Table 4.2.4 shows the preliminary results of the measurements of Full-Width Half Maximum (FWHM) of the PSF for the imaging bands of the IRC cameras in phase 3.

Table 4.2.4: Preliminary values of Full-Width Half Maximum (FWHM) of the PSF for the IRC NIR imaging bands for phase 3

(1)	(2)	(3)
Channel	Band	FWHM (pix)
NIR	N2	3.2
	N3	3.2
	N4	3.2

Chromatic Aberration

The NIR camera has chromatic aberration of 0.3–0.4 mm, which is in fact larger than the designed value. The most likely cause is the uncertainty of the optical characteristics of the elements under cryogenic temperature. The mean amount of aberration is comparable to that of the diffraction limited optics at 2 μm and thus effects the image quality.

Optical Transmittance

The throughout transmission functions (RSRF: Relative Spectral Response Function) of the IRC NIR broad band filters are shown in Figure 4.2.2. The filters and optical components as well as the detector response are taken into account to produce the curves[1]. These RSRFs can be

[1]These RSRFs have been prepared in collaboration with Dr. Martin Cohen to ensure a common calibration of the IRC with other missions and ground-based instruments, including Subaru/COMICS, in the framework of the absolute calibration network provided by him and his colleagues.

directly integrated over spectra given as F_λ to obtain the in-band fluxes (synthetic photometry). These RSRFs are derived for phase 2 observations. Minor changes are expected in phase 3.

Figure 4.2.3 shows the RSRFs of the dispersion elements (given per photon). These data are also available in digital format on the Observer's support web pages.

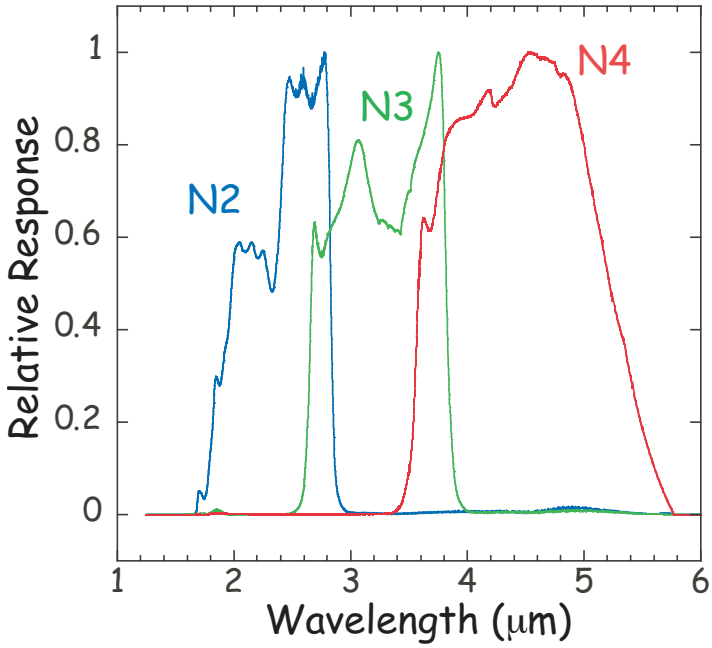

Figure 4.2.2: The Relative Spectral Response Function of the IRC/NIR Camera for F_λ.

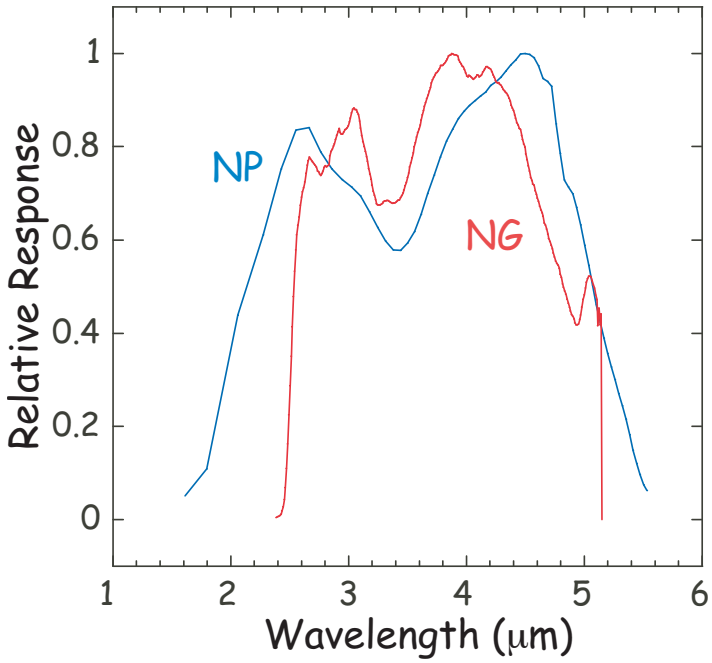

Figure 4.2.3: The Relative Spectral Response Function of the IRC/NIR dispersion elements per photon.

Distortion

Image distortion of the IRC NIR camera is negligible. The difference in the pixel scale in the X and Y directions is corrected in the data pipeline processing.

Ghosts

There are several ghost patterns recognized for the NIR data. They are noticeable only when bright sources are in the field-of-view. For details please refer to the IRC Data Users Manual.

4.2.2 Detector system

Hot Pixels

The number of hot pixels increased dramatically in phase 3. They are now about 5% of the total number of pixels and are more concentrated in the slit spectroscopy area (Figure 4.2.4). Software that treats these hot pixels is now available. Observers are strongly recommended to perform redundant observations.

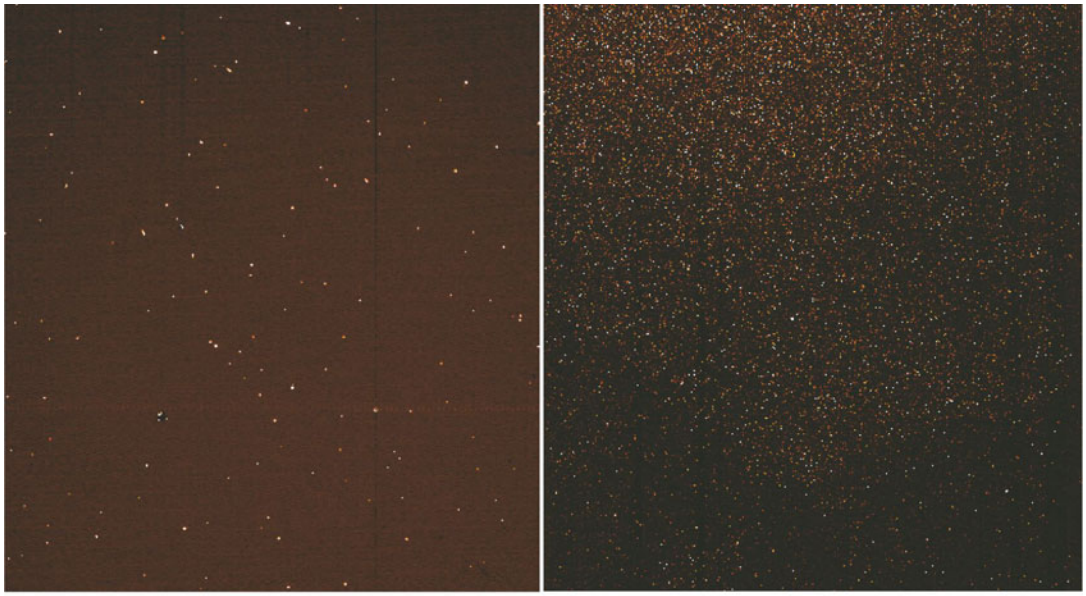

Figure 4.2.4: Dark frame images in phase 2 (a) and phase 3 (b) in the same ADU scale.

Linearity

The well-capacity of the NIR array is reduced by a factor of 5–6 in phase 3 compared to that in phase 2, because of the lower bias voltage used for phase 3 to reduce the number of hot pixels. Observers should be aware of the dramatic reduction of the saturation level in phase 3. Observations of bright sources will not provide meaningful data, although they will not make an aftereffect and thus will not be prohibited. The linearity correction below the saturation level set by the well-capacity will be made in the pipeline data processing.

Sensitivity

According to a preliminary study, the sensitivity (ADU to Jy) is reduced by 70% compared to the phase 2 performance. No appreciable change in the sensitivity during phase 3 has been noticed.

4.3 The IRC Instrument Operation

4.3.1 Pointed Observations

Exposure cycle

The minimum observation unit of the IRC is called an *exposure cycle*. An IRC pointed observation consists of an n times repeated *exposure cycle* with operations such as a filter change and Micro-Scan inserted between them. The operation sequence of the exposure cycle is designed by the IRC team to optimize the performance of the instrument and observation efficiency. The design of an exposure cycle is illustrated in Figure 4.3.5.

The unit time length for a detector driving is 2.3376 seconds, which corresponds to the time for the NIR detector to access all pixels in the array. Time durations in the exposure cycle are always a multiple of this unit time.

One exposure cycle takes 28× unit time (=65.4528 s). The NIR detector carries out one short (2× unit time = 4.6752 sec) and one long exposure (19× unit time = 44.4144 sec) in a cycle. The short exposure is useful for bright stars that may saturate the detector. However, the photometric accuracy of the short-exposure is worse than the long-exposure. *Fowler 4* sampling is taken for the longer integrations to reduce the readout noise by a factor of two.

Two images from the NIR channelare produced in one exposure cycle. They are stored in the frame memory buffer, then divided into telemetry packets and down-linked to the ground. The on ground data reformatting software will reconstruct the frame memory buffer and eventually a set of images, which are then passed to the observers.

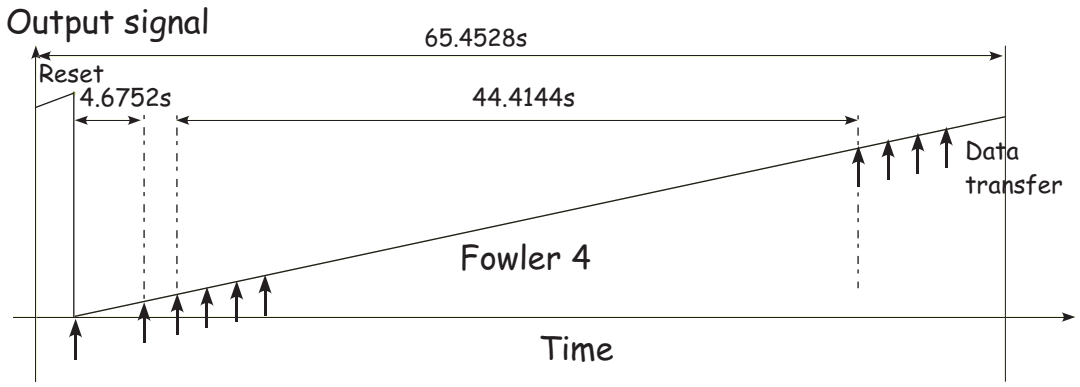

Figure 4.3.5: Illustration of the operation of one exposure cycle. A pair of short and long exposures are carried out for the NIR camera.The upward arrows indicate the data read timing.

A pointed observation is carried out by repeating the exposure cycle with Micro-Scans and filter changes inserted between them. These operations cause dead time due to the operations themselves and stabilization of the satellite attitude. The dead time is 20–80 seconds, depending on the operation and the performance of the attitude control system. Additional time for sending the data to the satellite's data processor (DHU) is also needed. These operations and dead-times are taken into account in the design of the Astronomical Observation Templates (AOT; section 4.4).

During a pointed observation, the IRC on-board controller communicates with the Attitude and Orbit Control Unit (AOCU) via the DHU. When the IRC requests a Micro-Scan for dithering, it asks the AOCU to perform the operation. The AOCU drives the satellite, then waits for the stabilization. When the AOCU decides that the satellite has stabilized, with a preset criteria, it sends back a signal to the IRC (via the DHU) to start the next exposure cycle. This

sequence continues until the AOT is completed. If, by some reason, the attitude of the spacecraft exceeds the allowed range of the angle with respect to the Earth, the AOCU stops the pointing mode attitude and returns back to the survey attitude, regardless of the observation. The IRC will continue its programmed exposure sequences but of course those data acquired during the maneuver are useless and will not be provided to the users. Current AOTs assume that one pointed observation could last longer than 10 minutes and add extra exposure cycles at the end.

4.4 The IRC AOTs

The Astronomical Observation Templates (AOTs) of the IRC are summarized in Table 4.4.5. Five AOTs are defined for the instrument.

Note that the actual AOT sequence has been modified from phase 2 and thus the designation of the AOT is changed from that used in phase 2. AOTs are now called Z# rather than 0#, where the same number # indicates the corresponding AOT in phase 2. The largest modification in the observation sequence consists in 5 dark frames before and after the actual observation to obtain information on the dark current for each observation. There are also more options (parameter combinations) available for each AOT.

Table 4.4.5: IRC AOTs and user parameters.

AOT	Purpose	# of filters per ch.	Dithering	Parameters	
				Filter	Pointing
Z0	Deep imaging	1	No	3 choices	N
Z2	Imaging with 2 filters/ch.	2	3 pos/filter	2 choices	N
Z3	Imaging with 3 filters/ch.	3	2 pos/filter	N/A (fixed)	N
Z4	Spectroscopy	1	No	2 choices	Ns, Np, Nh, Nc

The procedures for the AOT operations for IRCZ0, Z2, Z3 and Z4 are shown in Figure 4.4.6. As explained in the previous section (4.3.1) an AOT consists of a combination of exposure cycles (indicated as "exposure cycle"), Filter Wheel rotations ("W") and Micro-Scan operations ("M"). They are optimized such that the maximum exposure time is obtained. The AOTs are designed to use more than 600 sec in the case that extra observation time is available. The actual observation time depends on the stability of the target acquisition procedure.

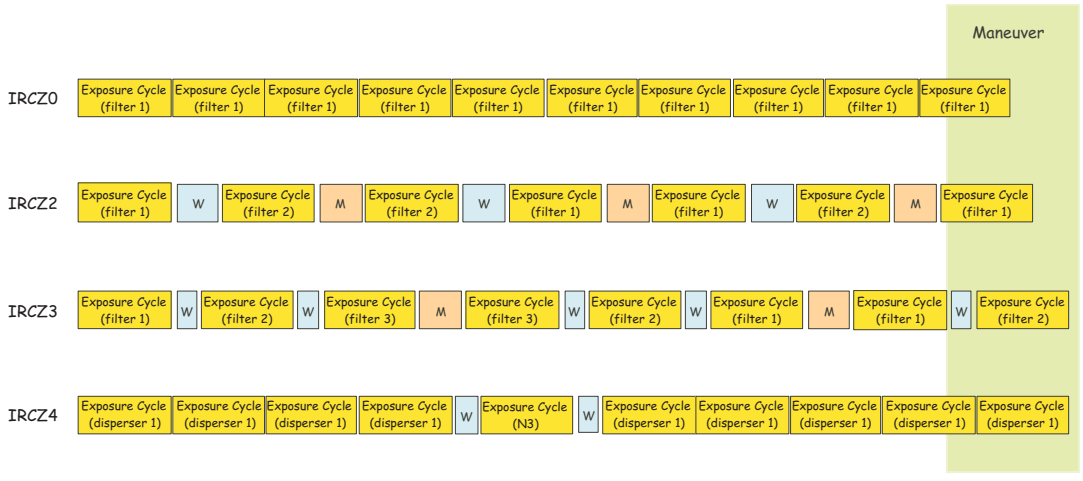

Figure 4.4.6: Observation sequences of the AOT IRCZ0, Z2, Z3, and Z4. Yellow boxes indicated as "exposure cycle" with filter / dispersion element names are exposure cycles. Orange boxes with "M" are Micro-Scan operations including stabilization, and light-blue boxes with "W" are Filter Wheel rotations. Dead time for a Filter Wheel change depends on the relative position of the elements. The Green area on the right side is the extra observation time which is not guaranteed. Note that for IRCZ2, filter 2 corresponds to NP when parameter "b" is specified.

4.4.1 Detection Limits and Saturation Limits: General Remarks

In the following sections, the expected detection limits for corresponding AOTs are given. These are 5σ detection limits per single pointing opportunity, extrapolated from the performance evaluated in phase 2 for relatively low-background sky (high ecliptic latitude regions) with the assumption that the detection limit is worse by a factor of 2 than in phase 2. The factor of 2 was derived taking into account the degraded PSF, the degradation in the sensitivity, and the noise level in phase 3, which provides the best estimate at the present. The detection limit for diffuse (extended) source is estimated from the point source detection limit, divided by the area given by the FWHM of the PSF (Table 4.2.4). Repeating an observation of the same region with the same AOT is supposed to improve the sensitivity by a factor of $\sqrt{n}$, where n is the number of pointing opportunities. **Since the number of hot pixels in the NIR detector is dramatically increased in phase 3, redundant observations are strongly recommended.**

The saturation limits are given as the flux level at which the detector signals deviate from linearity by 10 per cent. In fact, it is a rather rapid change from these levels to the absolute saturation and it is reasonable to use these levels as the saturation limits. The saturation limits are the same for all the imaging AOTs (IRCZ0, IRCZ2, and IRCZ3). The saturation limits for a short exposure are given in Table 4.4.6.

Table 4.4.6: Saturation limits for IRC imaging modes

Camera	Filter	$F_{\rm sat}$
		(Jy)
NIR	N2	0.13
	N3	0.11
	N4	0.07

4.4.2 IRCZ0: Deep Imaging Mode

Recommended Usage

IRCZ0 mode is prepared for deep imaging observations of high visibility regions where more than 6 pointed observations can be easily obtained.

Description

The mode is designed to maximize the exposure time during a pointing opportunity. The exposure cycle is simply repeated until the end of the pointed observation. No filter change nor dithering operation is inserted. It is expected that observations with other filter(s) and data redundancy by dithering are taken on additional pointing opportunities. It is strongly recommended to observe the same sky position with at least three independent pointings with the same filter setting. The necessary number of pointings is then multiplied by the number of filters. Therefore IRCZ0 is only applicable in very high visibility regions, at high ecliptic latitudes. It is recommended for observers to use this mode only in areas of the sky that can be observed more than 6 times (three dithers, two filters). Due to operational constraints it is very difficult to ensure such high visibility for Open Time and thus use of this mode has to be planned with great care. If the multiple observations are requested under the same target ID, small shifts of the pointing position among independent pointing observations (dithering operation among pointing observations) are automatically arranged in the scheduling software. Observers who wish to set the observation positions by themselves should specify the target position in each pointing opportunity and should not use multiple pointing assignments.

Parameters

Only the filter to be used can be specified as defined in Table 4.4.7. The FoV reference position is fixed at the center of the NIR camera (N).

Table 4.4.7: Filter parameter of IRCZ0

Parameter	a	b	c
filter	N2	N3	N4

4.4.3 Expected Performance

Detection Limits

The expected 5σ detection limits of the IRCZ0 observing mode are given in Table 4.4.8 assuming 9 exposure cycles for one filter in a pointing opportunity.

Table 4.4.8: Detection limits (5 σ) for AOT IRCZ0

Filter	Point source (μJy)	Diffuse source (MJy sr^{-1})
N2	18	0.036
N3	18	0.035
N4	18	0.035

Saturation Limits

The saturation limits of the IRCZ0 mode are given in Table 4.4.6.

4.4.4 IRCZ2: Imaging and Spectroscopy with Two Filters or Filter and Prism

Recommended Usage

IRCZ2 mode is prepared for general purpose imaging or spectroscopic observations. This mode can be used at any sky position even in low visibility regions.

Description

A sky position is observed with two filters each of which consist of three images with small position shifts by dither. i.e., this AOT can provide a self-standing data set in just a single pointing. The net exposure time per filter is about 1/3 of IRCZ0. The IRCZ2 provides a new imaging (N3) and prism (NP) mode in addition to the original IRC02 mode with two filters (N3 and N4). The spectroscopic mode provides an imaging and slit-less spectroscopic mode with dithering operation, which is different from IRCZ4. With the large number of hot pixels, dithering operation in one pointing could provide useful redundant information. On the other hand, it may reduce the accuracy in the determination of the reference wavelength position because of the dithering.

Parameters

There are two choices for the filter/disperser combination in this AOT as given in Table 4.4.9. The parameter *a* is set for imaging with N3 and N4 and *b* (new for phase 3) is set for N3 and prism.

Table 4.4.9: Filter combination of IRCZ2

Parameter	a	b
Filter/Prism	N3 & N4	N3 & NP

The FoV reference position is fixed at the center of the NIR camera (N).

4.4.5 Expected Performance

Detection Limits

The expected 5σ detection limits of the IRCZ2 imaging mode are given in Table 4.4.10, assuming 3 exposure cycles per filter in a pointing opportunity. The NP mode 5σ detection limit is shown in Figure 4.4.7.

Table 4.4.10: Detection Limits for IRCZ2

Filter	Point source	Diffuse source
	(μJy)	(MJy sr^{-1})
N3	31	0.061
N4	31	0.061

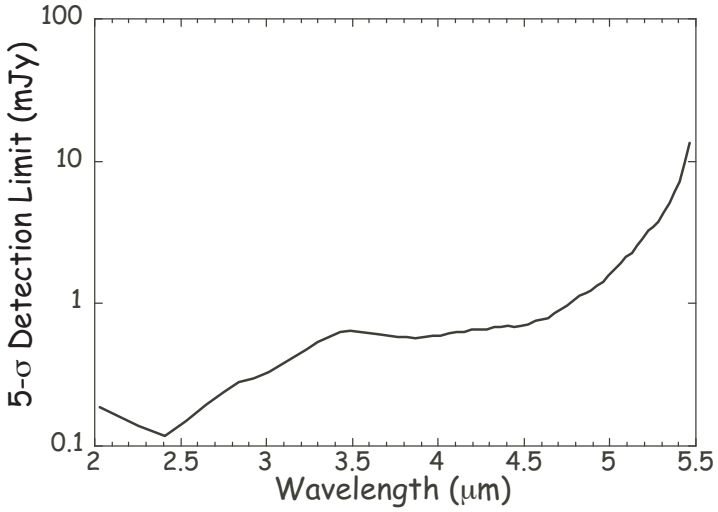

Figure 4.4.7: 5σ detection limit for NP in IRCZ2.

Saturation Limits

The saturation limits of the IRCZ2 imaging mode are given in Table 4.4.6. For the NP mode it is estimated to be about 3Jy at 3 μm. However the saturation in the N3 mode will make it difficult to determine the reference wavelength position from the N3 image accurately.

4.4.6 IRCZ3: Imaging with Three Filters

Recommended Usage

IRCZ3 is used for general purpose observing. It observes a target with all three filters of each camera. This mode is *not* recommended for sky areas of low visibility where two pointed observations cannot be guaranteed.

Description

IRCZ3 is similar to the IRCZ2 mode but differs in the number of filters and dithering positions in one pointing opportunity. The target sky position is observed by three filters. Instead, only one *Micro-Scan* (2 dithered images) is applied for each band. To obtain reliable results it is recommended to have sufficient redundancy by observing the same sky position at least twice on different orbits. The net exposure time per filter is thus 2/9 of the IRCZ0.

Parameters

IRCZ3 uses all filters of the IRC NIR channel. The advantage of using this mode over IRCZ2 has to be carefully considered from the scientific viewpoint of each observation. The position reference is fixed at the center of the NIR camera (N).

4.4.7 Expected Performance

Detection Limits

Expected 5σ detection limits of the IRCZ3 observing mode are given in Table 4.4.11, assuming 2 exposure cycles per filter in a pointing opportunity.

Table 4.4.11: Detection limits for IRCZ3

Filter	Point source	Diffuse source
	(μJy)	(MJy sr^{-1})
N2	39	0.076
N3	39	0.075
N4	38	0.075

Saturation Limits

The saturation limits of the IRCZ3 mode are given in Table 4.4.6.

4.4.8 IRCZ4: Spectroscopic mode

Recommended Usage

IRCZ4 is prepared for spectroscopic observations with the IRC. Observation with this mode can be made in regions of moderate to high visibility which allow two or more pointed observations at each target position.

Description

In this mode, the IRC dispersion elements are used to take spectra of the targets. The wavelength coverage of the NP (moderate resolution) and NG (high resolution) are similar to each other, and the user should choose one of these two for this AOT.

As we explain in section 4.1.5, a slit is provided in each camera in order to observe diffuse radiation. The NIR camera also has an entrance aperture (slit) for a point source, to enable confusion-less spectroscopy. It is used with the NG in high-resolution mode (see below). In phase 3 all the combinations of the slit selection are available both for NP and NG.

An image with N3 is taken for pointing alignment. No dithering operation is carried out during one pointing in this AOT. Observers are highly recommended to observe the same area of the sky on three or more independent orbits to ensure data redundancy. If the multiple observations with Np or Nh are requested under the same target ID, small shift along the slit among independent pointing observations are arranged automatically in the scheduling software. Observers who wish to set the observation positions by themselves should specify the target position in each pointing opportunity and should not use multiple pointing assignments.

Parameters

The first parameter specifies the dispersion element for the NIR camera.

Table 4.4.12: Dispersion element selection in IRCZ4

Parameter	a	b
Disperser	NP	NG

The second parameter gives the position reference for this AOT. It is more complicated than other AOTs because of the presence of the slits. Np and Nh are intended to be used with the NG, and others with the NP, although all the position reference parameters are allowed both for NP and NG. **It should be noted that for point sources Nh or Ns should not be used. The absolute pointing accuracy of *AKARI* does not guarantee that the intended point source be located on the narrow slit. Also usage of Nc with NG for slit-less spectroscopy is not recommended unless observers assure that the target will not be confused by surrounding faint sources.**

Table 4.4.13: Target position parameter for IRCZ4

Code	Description
Nc	The target position is placed at the center of the NIR (FoV).
Ns	The target position is placed at the common slit of the NIR and MIR-S.
Np	The target position is placed at the point source aperture of the NIR.
Nh	The target position is placed at the high-resolution slit of the NIR.

4.4.9 Expected Performance

Detection Limits

Figure 4.4.8 shows the 5σ detection limits for point sources with NP and NG in low sky background regions, assuming 8 exposure cycles in a pointing opportunity Note that for high background regions, such as star-forming regions, the detection will be limited by background fluctuation more severely than plotted in these figures. Figure 4.4.9 shows the 5σ detection limits for diffuse sources with the Ns slit with NP and NG in low sky background regions, assuming that the slit width and the FWHM of the PSF given in Table 4.2.4. For the Nh slit, the detection limit becomes larger by a factor of 5/3.

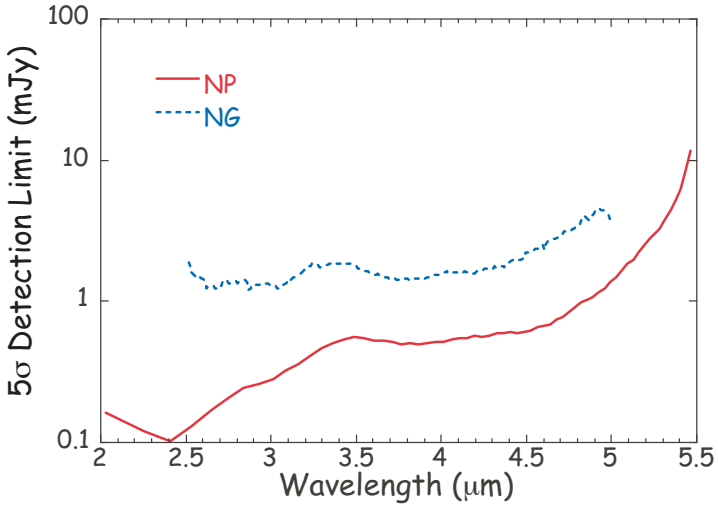

Figure 4.4.8: 5σ detection limits for point sources with NP or NG in IRCZ4.

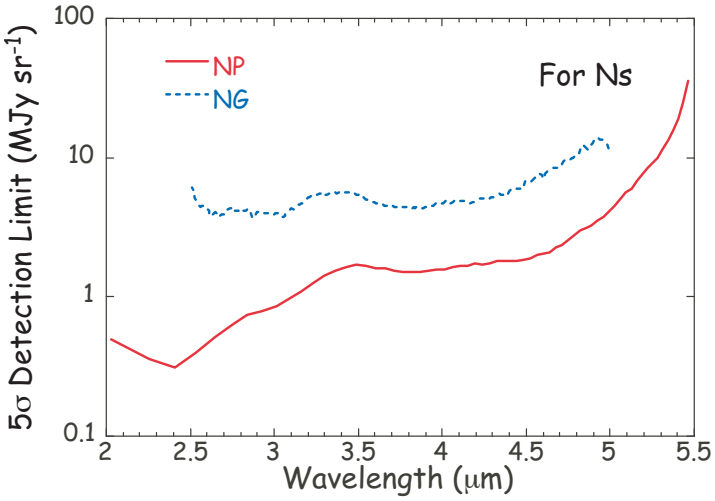

Figure 4.4.9: 5σ detection limits for diffuse sources with NP or NG in IRCZ4.

Saturation Limits

The saturation limits for NP and NG are about 3 and 10Jy, respectively. However, the saturation in the N3 imaging data sandwiched by spectroscopic observations could make it difficult to determine the reference wavelength position accurately for observations with Nc and Np. The saturation level for N3 is given in Table 4.4.6.

The NP works as a very broad band filter in the imaging FoV. Thus the background level becomes very high in high background regions. The low saturation level in phase 3 makes it very difficult to execute slitless spectroscopy with NP in high background regions, such as those near the Galactic plane. It should be noted that high background leaves only a few ADUs for point sources.

4.5 Notes and Restrictions for the IRC Observations

1. **Bright sources** Bright sources that saturate the NIR detectors will not leave significant effects on the following observations and thus will be planned not to be prohibited. However bright sources in the FoV can produce unwanted array anomalies, such as mux-bleed, and thus should be avoided as much as possible. Some constraint for observing fields with very bright sources may be given for IRC observations as observations progress.

2. **Effects of South Atlantic Anomaly (SAA)** Passage through the SAA does not cause serious damage to the detectors. However, detector performance may be significantly degraded immediately after the SAA. Current observation scheduling allocates IRC observations relatively close to the SAA region (say, 5 minutes after the passage).

Chapter 5

Data Reduction and Products

This section describes the data handling policy, current scope of the data reduction support and data products, particularly for phase 3 observations. Please note that the data reduction software is under development and only a preliminary plan is explained here. Details of the data handling and data reduction guide are prepared as Instrument Data User Manuals.

The data reduction steps for phase 3 IRC observations are performed in a similar manner to those for phase 2. However the very same software that is used for phase 2 data may not be applied. The software specific to phase 3 observations is currently being developed.

5.1 Basic Policy

The reduction of pointing observation data is the observer's responsibility. The AKARI team will provide the necessary information to handle the data, e.g., calibration data and software to correct instrument related characteristics. Astronomical analysis such as point source extraction should be carried out by commonly available software.

We welcome any users to participate in the data reduction activity at any level of the work, from giving quantitative reports of their data reduction results to proposing new algorithms to the programs.

5.1.1 IRC Data Reduction: AOT IRCZ0, Z2, Z3

IRC imaging mode data reduction is straightforward following a similar procedure to ground base observations. There are instrument specific corrections such as removing ghost images and spikes by charged particle hits.

Our support is limited to correction and calibration of each observation. We do not plan to support photometry of the calibrated images or mosaicing.

Currently the system is developed in the IRAF environment. Exporting it to IDL is TBD.

5.1.2 IRC Data Reduction: AOT IRCZ4

Data reduction of this mode is similar to that of the imaging mode for the basic processing of the dark subtraction, despiking, or bad pixel masking etc. In this AOT, an image is also taken with the N3 filter. Source positions are extracted from this image and applied to the spectroscopy images to clip each target.

Several relevant technical issues for the spectroscopic observations are listed below.

- For reliable spectroscopic observations we need accurate and wavelength dependent flat-fielding.
- Wavelength calibration is automatically made by the relationship between imaging position and the spectroscopy data. It also includes distortion correction of the image (Section 4.2.1).
- There may be confusion from nearby targets in the case of observations in crowded regions. Currently these are not decomposed but rather masked in the overlap region for the measurements.
- Measurement of the spectrum is carried out in an aperture on the spectroscopic image. The software attempts to fit an aperture automatically but the user may want to adjust this step interactively.

The tools are written in IDL.

5.1.3 Phase 3 data

Phase 3 data in the near-infrared channel suffer a number of hot pixels significantly. Also the dark current is no longer negligible. The operation sequence of phase 3 is different from that in phase 2 in taking the dark current measurements before and after the celestial observations. The associated dark measurements will be provided for the dark subtraction rather than the super-dark data provided in phase 2 data package.

Appendix A

AKARI Cookbook for Post-Helium (Phase 3) mission Open Time observations

A.1 Introduction

In order to aid observers with the preparation of proposals for Phase 3 Open Time, we present in this section three worked examples for observation and submission of Open Time proposals with AKARI. **Note that this chapter was originally prepared for the first year of Phase 3 as a guideline and descriptions with the first year should read as the second year.**

We show;

1. IRC Spectroscopy of distant galaxies with the NG grism in the point source aperture.
2. IRC Spectroscopy of a galactic target.
3. IRC Near-infrared imaging of extragalactic fields.

In general, the preparation of Open Time proposals follows the algorithm below, using dedicated tools available via a web interface. In addition, we expect users to iterate their observations using the tools before their final submission, in order to obtain the best possible observation strategy. Note that the tools available for Phase 3 Open Time are a scaled down and limited data set compared to those available in the earlier call. In particular, the Instrument Performance Tool (IPT) is not available for Phase 3 observation planning.

1. Target selection and visibility check
2. Preparation of the "Target list"
3. Validation check of the "Target list"
4. Run Duplication Check Tool
5. Submission via Submission Tool

A.2 Example 1: Spectroscopy of distant galaxies with the NG grism in the point source aperture

In this worked example we consider a program to carry out spectroscopy using the AKARI-IRC NG high resolution grism in the 1×1 arcmin point source aperture. We will simulate the preparation of the proposal from scientific background to proposal submission.

A.2.1 Scientific Background

The advent of the SCUBA instrument on the JCMT, Hawaii, allowed mapping of the sub-millimetre Universe for the first time. The first surveys detected a new population of dusty starburst galaxies, the high redshift analogue of local ULIRGs (Hughes et al. (1998), Smail et al. (1997)). Subsequent surveys have increased both in numbers of detected sources and areal coverage (e.g. Scott et al. (2002)) with the flagship being the SCUBA Half Degree Extragalatic Survey (SHADES, Mortier et al. 2005) covering 0.25 square degrees over two fields. The lack of any secure evolutionary picture of submm galaxies is partly due to fact that the observational results on submm galaxies are very limited. Until recently the only photometric data available for most of submm galaxies, was found mainly at NIR and submm wavelengths. This lack of photometric data has been alleviated somewhat with mid-infrared observations with Spitzer and AKARI although more detailed diagnostics on the observed diversi! ty and the evolutionary phase of these sources could be given by spectroscopic observations of a statistical sample of massive starburst galaxies. For example, the ratio of Hydrogen recombination lines can be used to estimate the extinction of starburst galaxies which may cause the observed diversity. Once the extinction is estimated from spectra, the extinction-corrected luminosity of the emission lines can be used to derive the SFR, independently of the observations of dust emission. Note that the SFR derived from submm fluxes depends on assumed dust temperatures, which are degenerate (Dunne et al. (2000)). Measurements of the extinction and the SFR from the emission lines, independent of the photometric data, are a key step to investigate the evolutionary phase of high-z massive galaxies. The measured extinction and SFR put a strong constraint on the SED model, which is used to investigate the evolutionary phase of starbursts linking them with the formation of spheroidal! systems. Current measurements of the near-infrared spectra of dusty s tarbursts have been limited to low redshift studies of local ULIRGS Veilleux (1997), Murphy et al. (1999), Dannerbaur et al. (2005). Our targets for the spectroscopy are the powerful Hydrogen recombination lines Paschen alpha at 1.875 micons and Paschen beta at 1.282 microns. Observations of the Hydrogen recombination lines in local ULIRGs (Dannerbaur et al. (2005)) have derived high Paschen alpha luminosities consistent with the predominant power source within these galaxies being star-formation rather than accretion from an AGN. Observations of a sample of higher redshift sources can test this measurement as a function of redshift. Note that at low redshifts ($z<<1$) both of the Hydrogen recombination lines lie outside the IRC grism observation window ($2.5 < \lambda < 5$ μm). For Paschen alpha the observable redshift range would be $0.3<z<1.7$, while for Paschen Beta it would be $0.95<z<2.9$.

The target galaxies are summarized in Table 1.2.1.

Table 1.2.1: Target sources for spectroscopic observations with AKARI

Name	Equinox	R.A.	Dec.
SMMJ030227 +000653	J 2000	03:02:27.73	+00:06:53.5
SMMJ163639 +405635	J 2000	16:36:39.01	+40:56:35.9
SMMJ123549 +621536	J 2000	12:35:49.44	+62:15:36.8
SMMJ221733 +001352	J 2000	22:17:33.91	+00:13:52.1

A.2.2 Selection of Targets and Target Visibility

A Visibility Tool is provided that gives an approximate estimation of the open time visibility of the target field during the Phase 3 of the AKARI mission, assuming an observation period of October 2009 to October 2010. The following constraints are imposed on the target visibility;

1. The instrument is of 10 arcmin width and at the boresight.
2. The maximum number of observations in a day is about 20, since 30% of the total number of pointings with AKARI are reserved for Open Time which translates roughly into 6 orbits every day or almost a degree interval on the ecliptic longitude
3. The same constraints on the SAA, Moon, and the number of stars in STT as in the first call will be applied.
4. The offset angle to the nominal scan path along the great circle constraint will be relaxed from 0.6 degree (but will still be smaller than the maximum 1 degree to ensure a safety margin for scheduling.)
5. The maximum number of pointed observations at any single pointing has a ceiling set at 50.

In addition to the above, any orbits not scheduled for the Mission Programs are available for *scheduling* for open time. However, visibility for specific targets is quite heavily constrained and an extremely strong function of ecliptic latitude. Targets in the ecliptic pole regions are observable ona large number of orbits, while targets near the ecliptic plane are visible by AKARI for only two days (30 orbits, i.e. 14.4 revolutions per day) in a half year at the most.

The Visibility Tool can be found on the AKARI Phase 3 AO page.

The visibility tool front end is shown in Figure 1.2.1. We have to provide a target list or a single pointing. The input coordinates and equinox shall be in the format HH:MM:SS.S (for J2000) or in degrees (for J2000, Ecliptic or Galactic).

Although it is not necessary to enter any information on the AOT into the Visibility Tool itself, at this stage, the visibility tool does take its input in target list format (see table 1.2.2).

The output for our target list is shown in Figure 1.2.2 which lists the query input on the right of the screen and the total number of allocations possible on the left.. position in Ecliptic coordinates, visibility in Phase 3b1 (2008 Oct. 15 – 2009 Apr. 11 = 179d), Phase 3b2 (2009 Apr. 12 – 2009 Oct. 14 = 186d) and the total visibility in Phase 3 (2008 Oct. 15 – 2009 Oct. 14 = 365d). In our case three of our sources are observable for an adequate number of slots. However, one of our targets (SMMJ030227 +000653) is only observable on four opportunities. In this particular case it is a combination of the low Ecliptic latitude and a significant number of pointing opportunities lost to interference from the South Atlantic Anomaly (SAA). This emphasizes the strong constraint on the visibility imposed by the orbit of AKARI on the scheduling of observations. We will therefore drop SMMJ030227 +000653 from our target list.

The output from the visibility tool should be saved as an ASCII file as it will need to be uploaded as part of the final submission process for our proposal.

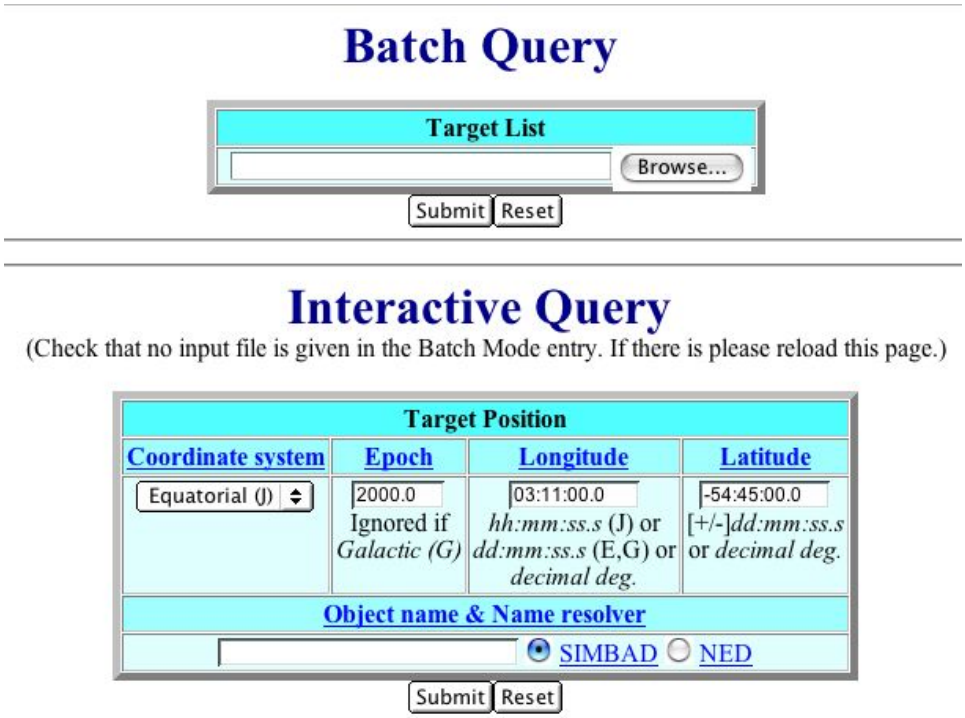

Figure 1.2.1: The Visibility Tool user front end for Phase 3 observations.

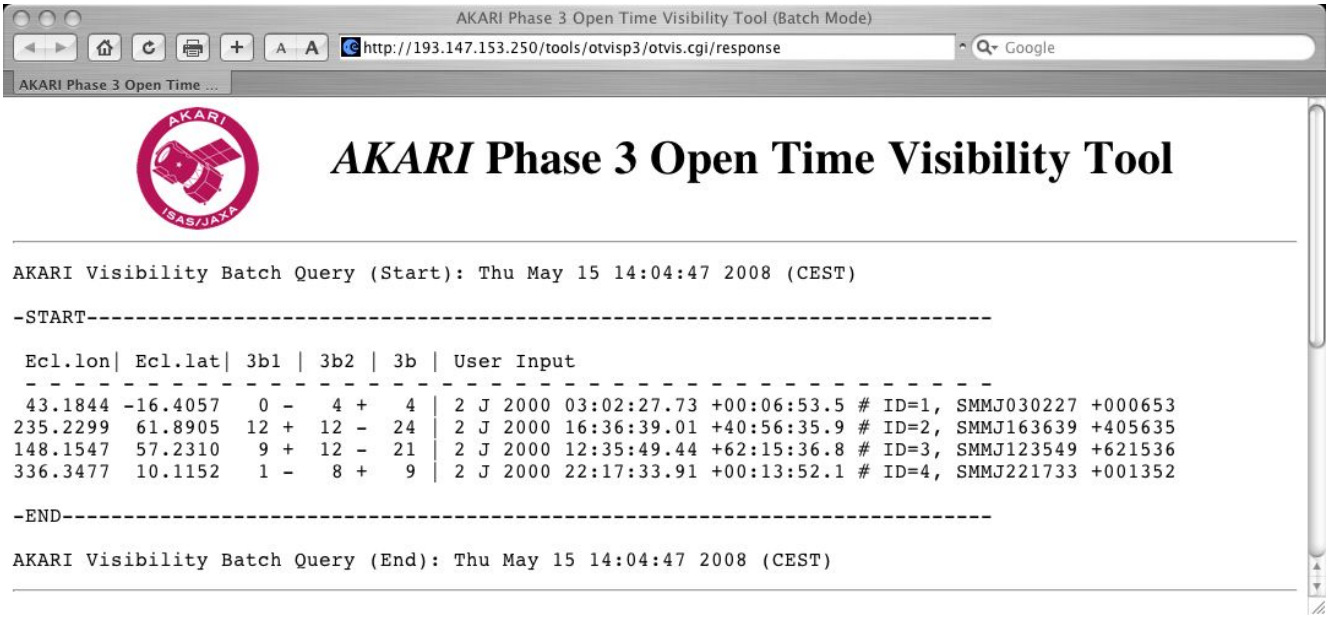

Figure 1.2.2: Results from the Visibility Tool in batch mode. The result shows the total number of allocations possible during Phase 3 of the AKARI mission. Each target is listed by position in Ecliptic coordinates, visibility in Phase 3b1 (2008 Oct. 15 – 2009 Apr. 11 = 179d), Phase 3b2 (2008 Apr. 12 – 2009 Oct. 14 = 186d) and the total visibility in Phase 3 (2008 Oct. 15 – 2009 Oct. 14 = 365d). The original user input is shown on the right.

A.2.3 The Choice of Observation Mode

AKARI provides four reasonable methods for spectroscopy of distant galaxies.

- Slitless spectroscopy in the main 10×10 arcmin field of view using NP prism.
- Slitless spectroscopy in the main 10×10 arcmin field of view using NG grism.
- Slit spectroscopy using the NP prism in the 1×1 arcmin point source aperture.
- Slit spectroscopy using the NG Grism in the 1×1 arcmin point source aperture.

Observations using the slits (Nh,Ns) are not appropriate for point source observations (due to insufficient pointing accuracy) and should be avoided. The slitless spectroscopy with AKARI using the NP prism creates low resolution spectra over the entire field of view of the imaging plane. However, to obtain the sensitivity using NP to detect the contiuum of most distant sources we would have to integrate so far down that we would run into source confusion problems with multiple overlapping source spectra. The confusion problem with the NG grism in slitless mode is compounded by an even bigger wavelength dispersion (more overlapping sources). For the detection of lines, using the 1×1 arcmin point source aperture, the resolution of the NP element is too low. Therefore we find that indeed slit spectroscopy using the high resolution grism on the IRC is the most efficient method to observe our distant galaxies.

Current estimates of the detection limit for lines in Phase 3 compared to the earlier phases of the mission assumes a degradation of at least a factor of two and there is still a great deal of uncertainty surrounding the actual values. For the proposed NIR spectroscopy with AKARI in the 2.5–5μm range by using the IRC grism, a line sensitivity of $\sim 5\times10^{-18}\mathrm{Wm}^{-2}$ for a 10 minute integration is achieved. In Figure 1.2.3 we show the predicted line strengths for the Hydrogen recombination lines Paschen $\alpha\&\beta$ as a function of redshift assuming an ultra-luminous infrared galaxy similar to our targets with an infrared luminosity of $5\times10^{12}\mathrm{L}_{\odot}$. In general we may require between 8 to 10 pointings to detect our sources at z>1.

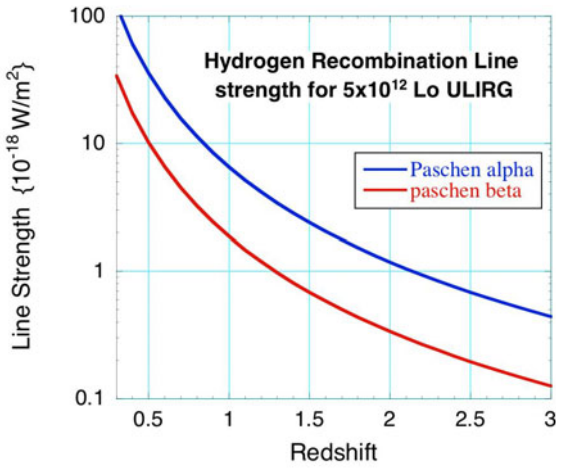

Figure 1.2.3: Predicted Hydrogen recombination line fluxes for a $5\times10^{12}\mathrm{L}_{\odot}$ Ultraluminous Infrared Galaxy.

A.2.4 Preparation of Target List

The objective of our IRC observations is to detect the Hydrogen recombination lines in dusty, distant galaxies. as explained in the previous section, the optimum instrument configuration for this objective is to use the IRC in NG grism mode with our target located in the point source aperture (Np). Thus we require the following AOT parameters;

- AOT : IRCZ4 (note the insertion of the "Z" in the original AOT name for Phase 3)
- Parameter 1: b (corresponding to the grism NG)
- Parameter 2: Np (The target is placed in the point source aperture of the NIR channel)

Our estimates for the required sensitivity for the detection of the target lines are between 8-10 pointings per target. We conservatively select 10 pointings per source since the visibility constraints are not harsh. Not that the number of hot pixels in the IRC-NIR camera have also increased dramatically in Phase 3 of the mission and a large number of pointings is important to ensure adequate dithering of our observations.

Now the appropriate AOT has been selected, we can go ahead and prepare the target list for our observations. An AKARI target list contains one line per target per AOT per field of view. Since we are only observing our target fields with the IRC-NIR-NG grism, we will have four lines in our target list, one per target galaxy. The target list is shown in Table 1.2.2. The target list consists of a unique I.D. in ascending but not necessarily contiguous order, followed by some identifier for the target name which should if possible be a resolvable by systems such as SIMBAD, NED. The next 3 fields are reserved for the coordinate system and target coordinates. we enter these in "`J2000`" equatorial coordinates in the `HH : MM : SS.S` format although degrees are also acceptable. Coordinates entered in "`ecliptic`" format should b in decimal degrees.

Next we need the AOT, which will be IRCZ4. Following the AOT are the specific parameters for each given AOT. For the IRC, we have to specify 2 parameters, the filter combination (prism or grism) and the aperture (main field of view or one of the aperture / slits) with which we want to observe. We intend to observe with the NG grism in the point source aperture - so we can fix the first parameter as *b* and the second parameter as *Np*, i.e. *b;Np*.

In the following field we input the number of pointings for each AOT, for our case this will be 10 for each target. We then have to prioritize our targets. AKARI Open Time Observations are divided into 3 priorities, A , B, C . Our A & B targets, barring any unforeseen events, should be observed, while the priority C targets should be considered as back-ups. In our target list, the number of priority A , B, targets should be around the same and the number of C target should be roughly $A + B$. For our observations therefore we allocate one priority A target, one B and the remaining target as priority C .

Note: It is extremely important to include an ample number of C targets (even though we have not done so in this particular example) as AKARI scheduling is tough and if there are not enough back up targets you may lose your allocation. A good size number of priority C targets is also necessary to replace any higher priority targets that may incur possible duplication conflict (see the discussion on duplication later) with Mission Program targets.

Field 10 (symbiotic) is not used in phase 3 scheduling. Just leave the field blank – not forgetting the "comma" field separator. Finally, any notes are appended on the end of each target list line. Our final target list is shown in Table 1.2.2.

Table 1.2.2: Target List for submission

2, "SMMJ163639 +405635", "J2000", 16:36:39.01, +40:56:35.9, "IRCZ4", "b;Np", 10, A, , "redshift 1.488"
3, "SMMJ123549 +621536", "J2000", 12:35:49.44, +62:15:36.8, "IRCZ4","b;Np", 10, B, , "redshift 2.2032"
4, "SMMJ221733 +001352", "J2000", 22:17:33.91,+00:13:52.1, "IRCZ4", "b;Np", 10, C, , "redshift 2.5510"

A.2.5 Target List Validation

Once the target list has been completed, we can proceed towards the submission stage. However there are still a few steps to complete. We should run our target list through both the Target List Validation Tool and then we need to submit the target list to the observation Duplication Check Tool.

The Target List Validation Tool takes a target list and makes a simple check on the target list format, e.g. correct number of fields, AOT in expected form etc. It does not perform any test on the scientific validation, e.g. on position or sensitivity etc. We can submit the Target List as a batch file in a similar manner to the Visibility Tool as in Figure 1.2.4, in fact this (target list) format is accepted by all tools during the submission process. Figure 1.2.5 shows the output of the Target List Validation Tool. Any errors are highlighted in red and a summary given at the bottom of the output. In this case an AOT has been input incorrectly and has been highlighted. The target list should therefore be edited and re-submitted.

The target list will be automatically validated when we upload it during the final proposal submission stage so there is no need for us to save the output of the Validation Check Tool.

Figure 1.2.4: Input to the Target List Validity Checker

```
2, "SMMJ163639 +405635", "J2000", 16:36:39.01, +40:56:35.9, "IRCZ4", "b;Np", 10, A, , "redshift 1.488"

3, "SMMJ123549 +621536", "J2000", 12:35:49.44, +62:15:36.8, "IRCZ4","b;Np", 10, B, , "redshift 2.2032"

4, "SMMJ221733 +001352", "J2000", 22:17:33.91,+00:13:52.1, "IRC10", "b;Np", 10, C, , "redshift 2.5510"
# AOT name does not exist (options are: IRCZ0, IRCZ2, IRCZ3, IRCZ4)

### Pointings ... Total=20 : S=0 A=10 B=10 C=0 D=0
### Format error=1
```

Figure 1.2.5: Output from the Target List Validation Tool. Any Errors are marked in red and the number of errors are listed at the bottom of the output in the Pointings summary. In this case an AOT has been input incorrectly.

A.2.6 Duplication Check

Duplicate observations are decided on a basis of position, instrument/AOT and the number of pointings. Figure 1.2.6 shows the input screen for the Duplication Check Tool.

This tool returns all IRC observations within a radius of 5 arcmins from the requested targets, which are either executed in the cold phase (Phase 1 and 2), or are in the blocked target list for Phase 3. The observations executed in the cold phase are in the public domain at the time of Phase 3 Open Time. A strict duplication occurs when AOT and parameters of a requested target are identical with those of a Phase 3 observation. The other cases returned by the tool may have to be discussed in the proposal scientific justification.

The output from the duplication tool is shown in Figure 1.2.7 and we can see that all our targets pass the Duplication Tool successfully. The output from the Duplication Check tool should be saved as an ASCII file as it will need to be uploaded as part of the final submission process for our proposal.

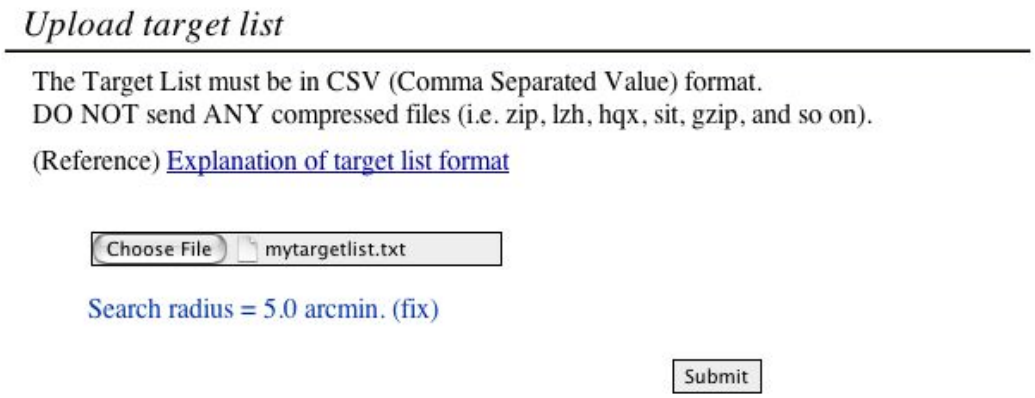

Figure 1.2.6: Input screen for the Duplication Check Tool. The input is the target list as usual.

Query : target list: S=0, A=10, B=10, C=10, D=0 (total=30), search radius = 5.000 arcmin.

0 targets in your list are duplicated with the blocked target list.

ID	R.A.	Dec.	AOT	Target name	Result
2	249.163	+40.943	IRCZ4,b;Np	SMMJ163639 +405635 (A)	OK
3	188.956	+62.260	IRCZ4,b;Np	SMMJ123549 +621536 (B)	OK
4	334.391	+0.231	IRCZ4,b;Np	SMMJ221733 +001352 (C)	OK

Command executed on 2008/05/15_22:31:50 (JST).

Figure 1.2.7: Output from the Duplication Check Tool for our target list. All our targets pass the Duplication Tool successfully.

A.2.7 Submission of Proposal

After the duplication check, we can finally submit our proposal via the web interface. The proposal submission has several stages and we will need to upload various output files saved from the tools we used earlier. Each proposal has a 5 character abbreviation which will be used to identify each proposal. The next step is to upload the Target List which will be automatically verified (syntax only) on uploading. Following this we will be required to upload the results we saved from the output of the Visibility Tool and Duplication Check Tool respectively. Once all these files have been uploaded we will have to enter the specific proposal information (name, address, telephone number, etc.) and general proposal information (Co-Is, category, title, abstract). The Scientific Justification must be submitted in PDF format and should not exceed 6 pages in total including scientific rationale, objective, references, figures and tables, and technical feasibility of the proposal. A confirmation page of the submission is created automatically. Shortly after, users will receive a formal confirmation by e-mail with the cover page of their proposal.

A.3 Example 2: Spectroscopy of Planetary Nebulae with the IRC

In this worked example we consider a program to perform spectroscopy on a few Planetary Nebulae with the AKARI IRC instrument. We will simulate the preparation of the proposal from scientific background to proposal submission.

A.3.1 Scientific Background

We consider 2 planetary nebulae as a study for spectroscopy with AKARI. These objects have extremely rich and highly ionized spectrum due to their hot central star. Analysis of the spectra can give insight into the evolution and origin of the ionizing central stars. Our first target is NGC7027, a very well known, bright planetary nebula with a rich spectrum that has previously been observed by ISO (Bernard-Salas et al., 2001). The second target is the fainter SMP83 planetary nebula in the Large Magellanic Cloud, also observed by Spitzer (Bernard-Salas et al., 2004). We will perform both high and lower resolution slit spectroscopy in the near-infrared range which is unique to AKARI, since Spitzer has no capability in this wavelength range. The target positions are given in Table 1.3.3.

Table 1.3.3: Suitable Planetary Nebula for Phase 3 spectroscopic study with AKARI

Name	Equinox	R.A.	Dec.
NGC7027	J 2000	21:07:01.7	+42:14:11.0
SMP83	J 2000	05:36:21.0	−67:18:14.0

A.3.2 Target Visibility

Using the Visibility Tool to check the availability of our targets (entering the coordinates using the interface in Fig1.2.1) we find that both targets have reasonable visibility. The result of the Visibility Tool for is shown in Figure 1.3.8 and 1.3.9 for NGC7027 and SMP83 respectively

Figure 1.3.8 shows that NGC7027 is visible only twice from October 2008 to April 2009 and a further 13 times in the latter half of Phase 3 (April 2009 - October 2009). This low visibility is mainly due to conflict with the SAA even given the reasonable ecliptic latitude.

Note the much higher visibility of SMP83, shown in Figure 1.3.9 due to its location almost on the South Ecliptic Pole at an ecliptic latitude of -87 degrees, compared to NGC7027 at a more moderate ecliptic l atitude of 55 degrees. This shows the huge advantage in scheduling gained by targets at extreme latitudes.

The output from the visibility tool should be saved as an ASCII file as it will need to be uploaded as part of the final submission process for our proposal.

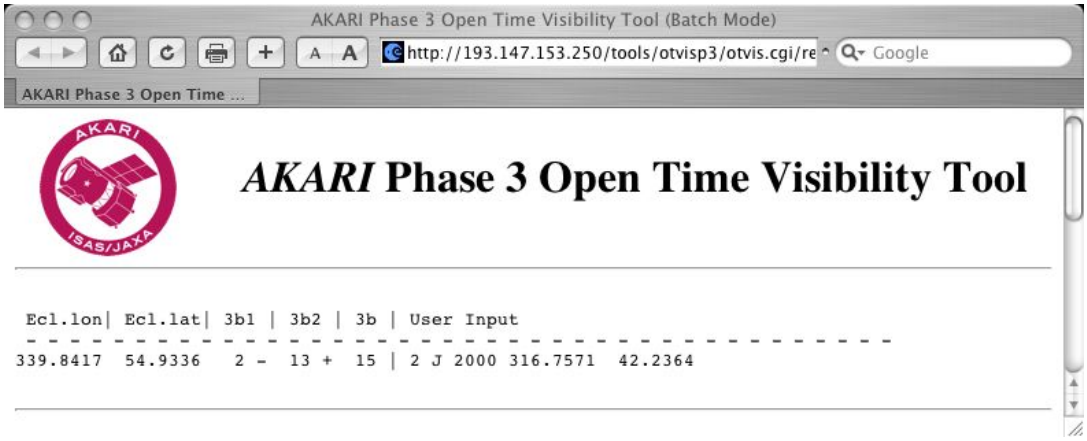

Figure 1.3.8: Results from the Visibility Tool in single target mode for the planetary nebula NGC7027. The result shows the total number of allocations possible during Phase 3 of the AKARI mission. Each target is listed by position in Ecliptic coordinates, visibility in Phase 3b1 (2008 Oct. 15 – 2009 Apr. 11 = 179d), Phase 3b2 (2009 Apr. 12 – 2009 Oct. 14 = 186d) and the total visibility in Phase 3 (2008 Oct. 15 – 2009 Oct. 14 = 365d). The original user input is shown on the right.

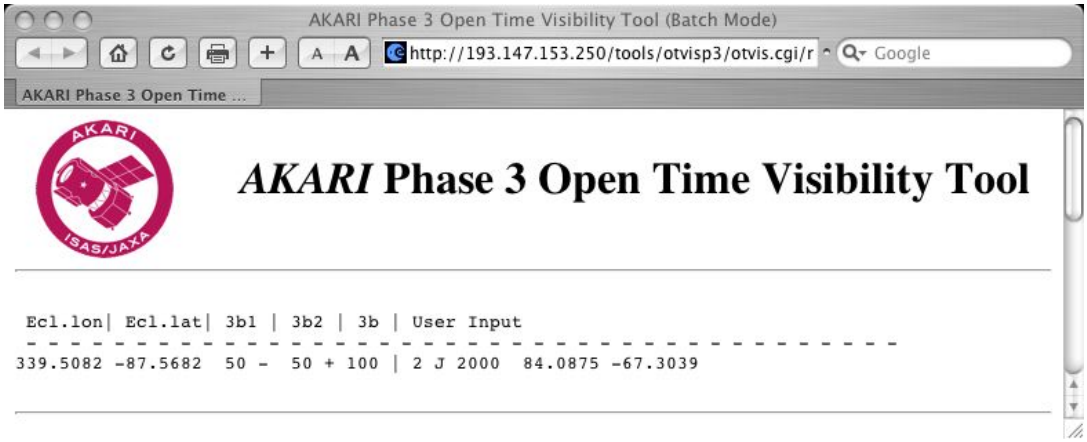

Figure 1.3.9: Results from the Visibility Tool in single target mode for the planetary nebula SMP83.

A.3.3 The Choice of Observation Mode

The estimated sensitivity of the IRC in slit spectroscopy mode during the "cold" phase of the IRC mission was around a few $\times\ 10^{-18}$Wm^{-2}. For Phase 3 we can expect at least a factor of two degradation in this sensitivity, to for example $5\times\ 10^{-18}$ Wm^{-2}. The near-infrared spectra of planetary nebula are rich Hydrogen and Helium lines and some ions such as MgIV, etc. For our first target (NGC7027) all the lines are brighter than 10^{-15} W m^{-2} (Bernard-Salas et al., 2001), therefore this is well above the IRC detection limits and should be easily observable in a single pointing. For our second target (SMP83) as a first approximation, we can scale the line fluxes of NGC7027 by the distance to the LMC. Under this assumption, we could expect the H2 line at 2.8 microns to be of the order of $\sim 3.0 \times 10^{-17}$ W m^{-2} and the Br alpha line at 4.05 microns to be $\sim 92.0 \times 10^{-17}$ W m^{-2}. A non-exhaustive list of example brighter line strengths estimated for SMP83 is given in Table 1.3.4. Fainter lines (e.g. He I 4-6, H I 6-15, 6-17 transitions) are of the order of 10^{-18} W m^2, and maybe be more difficult to detect at the IRC line detection limits.

Note that the saturation level for the NIR detectors is also significantly degraded for AKARI Phase 3 observations. For the grism and prism we could expect saturation limits of as low as $\sim\ few \times 10^{-15}$ W m^{-2} which may pose problems for our brighter lines. In addition there is a degradation in the saturation level of the continuum of around a factor of 5. This is important since the N3 imaging data taken in IRCZ4 is necessary to determine the wavelength origin. A rough estimation of the flux level that can be expected can be calculated by assuming an unresolved line with Flux F_l (W/m62) without continuum, where the dispersion elements works like a narrow band filter and we get the image on the detector just like the imaging mode. The line flux can be roughly converted to the 'continuum equivalent flux density' per pixel, F_c as, $F_c/pixel = (F_l \times 10^{26}/PSF^2)/d\nu$ Jy. Where dν is estimated from the instrument element resolution (i.e., dλ = 0.06 & 0.0097 for NP and NG respectively) in μm / pixel at 3.5μm. For NGC 7027 most lines are brighter than 10^{-15} W m^{-2} giving a corresponding continuum flux of 6.7 mJy & 42 mJy for NP and NG respectively. The saturation level of the N3 band is 110 mJy Note that this image does not have to be a particularly high quality image,and even if some portion of it is saturated, it may still be possible to estimate the wavelength scale.

Table 1.3.4: SMP83 line strengths

Wavelength (microns)	Line	Flux $10^{-17}W/m^2$
2.8	H2	3.0
2.626	Br β	46
3.74	Pf γ	11.0
4.05	Br α	92
4.654	Pf β	11.0

Concentrating on just the brighter lines in both nebulae, we can see the IRC is sensitive enough to detect these lines in SMP83 in a single pointing. Although we still require at least 3 pointings for dithering (see below).

A.3.4 Preparation of Target List

We intend to carry out high resolution slit spectroscopy with the IRC grism (NG) in the near-infrared as our first priority. Following this, as our second priority, we will observe the same dust spectrum at a lower resolution using the IRC prism (NP).

The spectroscopic IRC AOT for Phase 3 is IRCZ4. This AOT has 2 parameters, the first is the filter set and the second is the position of the slit. The NIR camera has 3 slits. A common slit with the IRC MIR-S camera for spectroscopy of diffuse sources using the NP element, an entrance aperture for point source spectroscopy and another slit for high resolution spectroscopy with the NG element.

We wish to carry out both high resolution spectroscopy with the NG element at the and lower resolution spectroscopy with the NP element, so we require an entry in the target list for both sets of observations for each target, making a total number of four lines in our target list.

In addition since no dithering is carried out during this AOT, we must observe each sky area at least three times for data redundancy. Therefore we are looking at a minimum of 3 pointings per target per observation mode. For our fainter target (the high visibility SMP83) we will decide to double the number of pointings to ensure high signal to noise detection of our lines. The complete target list is shown in Table 1.3.5.

Table 1.3.5: Target List for submission

1,"NGC7027","J2000", 21:07:01.7, +42:14:11.0,"IRCZ4","b;Nh",3,A,"","NGC7027 high resolution"
2,"NGC7027","J2000", 21:07:01.7, +42:14:11.0,"IRCZ4","a;Ns",3,C,"","NGC7027 lower resolution"
3,"SMP83","J2000", 05:36:21.0, -67:18:14.0,"IRCZ4","b;Nh",4,B,"","SMP83 high resolution"
4,"SMP83","J2000", 05:36:21.0, -67:18:14.0,"IRCZ4","a;Ns",4,C,"","SMP83 lower resolution"

As in the previous example, the target list comprises of a unique I.D. in ascending but not necessarily contiguous order, followed by some identifier for the target name which in the case of many of our targets should resolvable the NED/SIMBAD systems. The IRCZ4 AOT has 2 parameters to set, the filter set and the slit position. The filter set is determined by whether we wish to use the NP (filter set *a*) or NG (filter set *b*) element of the NIR camera. A tool (iris_sky) is provided to aid us with the positioning of the instruments over our fields. With it, we can project our instrument arrays onto our target fields (on images from IRAS and 2MASS). With iris_sky it is also possible to create our target list in its' entirety although we shall construct ours manually in this case. The use of iris_sky has been decribed in Version 3.2 of the Observers manual including an example in the cookbook. iris_sky has been modified for Phase 3 of the AKARI mission.

The FIS and IRC/MIR information has been removed from the Target list editing panel and messages amended accordingly.

Only the IRC-NIR detector is shown on the display by default (other detectors can be switched on via the options panel).

Detector positions are updated from the 'nominal' position in the Observer's Manual, to be relatively consistent with the images.

We can use the iris_sky tool to visualize our observations and Figure 1.3.10 shows the iris_sky tool with the outmost slit of the IRC-NIR camera positioned over the target (NGC7027). In this figure, the entrance aperture for point sources and the common inner slit for diffuse sources can also be seen.

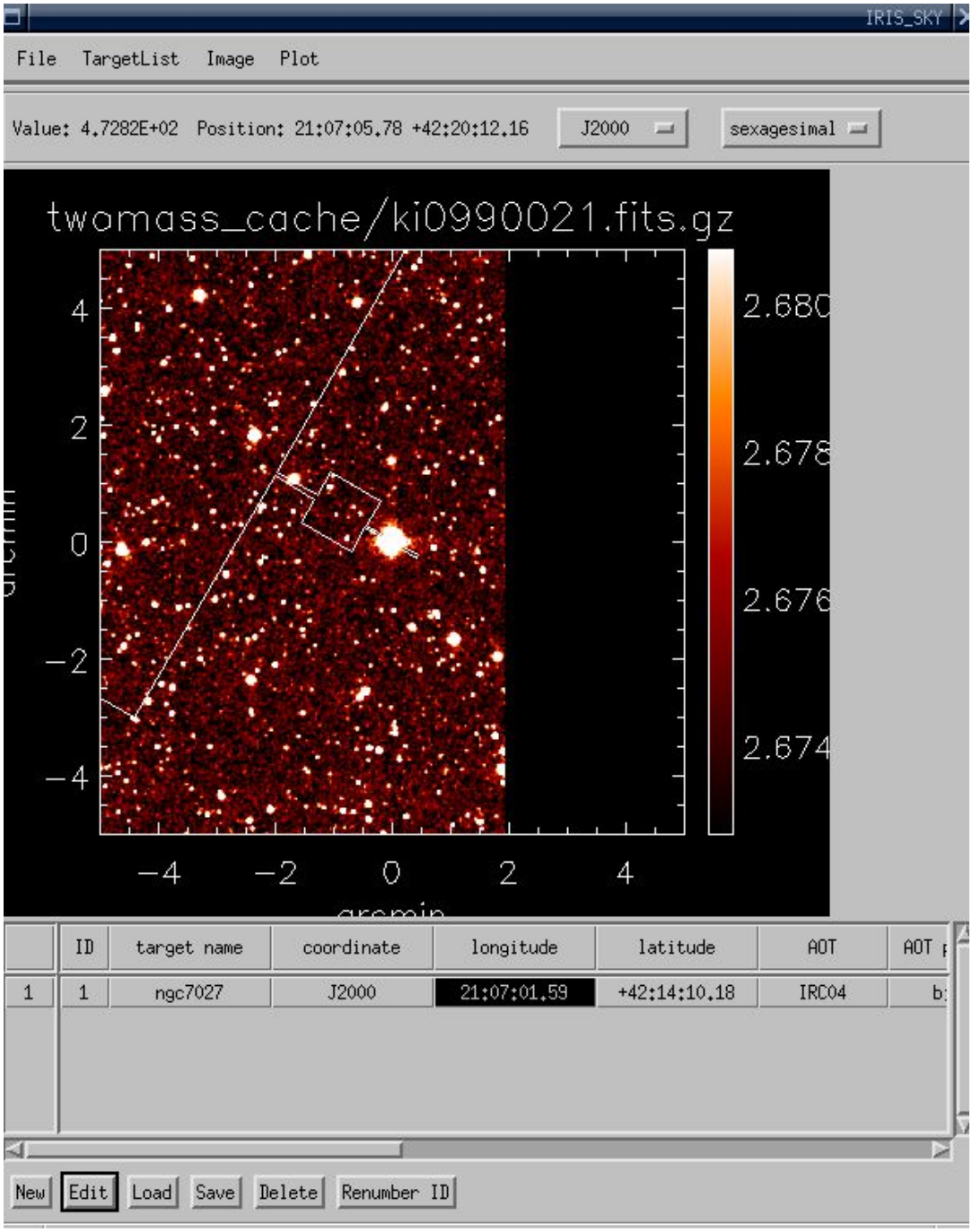

Figure 1.3.10: Using the iris_sky tool to overlay the IRC NIR high resolution spectroscopy slit (Nh) over the Planetary Nebula NGC7027.

Next we have to choose the slit parameter. For the high resolution spectroscopy, this parameter is *Nh* : the target position is placed at the high resolution slit of the NIR camera. For the lower resolution spectroscopy, the parameter is *Ns*. We set the number of pointings as 3 for the brighter source and 4 for our fainter source. For this example, we prioritize our targets by the high and low resolution spectroscopy, giving thigh resolution observations with NG a priority *A* & *B* and the lower resolution spectroscopy with NP priority *C* respectively.

A.3.5 Target List Validation

The Target List syntax is validated in an identical manner to the previous example in Section A.2. The target list will also be automatically validated when we upload it during the final proposal submission stage so there is no need for us to save the output of the Validation Check Tool at this stage.

A.3.6 Duplication Checker

Duplicate observations are decided on a basis of position, instrument/AOT and the number of pointings. The Duplication Tool returns all IRC observations within a radius of 5 arcmins from the requested targets. Putting our target list into the duplication checker we find that indeed there is a conflict of position for both of our targets (see Figure 1.3.11). Although the targets are indeed duplicated with a previous program during Phase 2 and another program planned for Phase 3, the AOTs are slightly different and it my fall to the responsibility of the Telescope Allocation Committee's interpretation of our scientific justification as to whether we can observe our targets! The output from the Duplication Check tool should be saved as an ASCII file as it will need to be uploaded as part of the final submission process for our proposal.

A.3.7 Submission of Proposal

After all the tools have been used and the Target List checked, we can finally submit our proposal via the web interface in an identical manner as that described for the previous imaging example in SectionA.4. Remember that we will need to upload the previously saved ASCII files from the outputs of the Visibility and Duplication Tools.

Query : target list: S=0, A=2, B=4, C=6, D=0 (total=12), search radius = 5.000 arcmin.

4 targets in your list are duplicated with the blocked target list.

ID	R.A.	Dec.	AOT	Target name	Result
1	316.757	+42.236	IRCZ4,b;Nh	NGC7027 (A)	Duplication (2)

# ID	R.A.	Dec.	AOT	Target name	d(') status
# 4081016	316.757	+42.236	IRC04,b;Ns	NGC7027 (CERN1,B)	0.0 Observed
# 1740550	316.757	+42.236	IRCZ4,b;Np	NGC 7027 (AGBGA,B)	0.0 Scheduled

ID	R.A.	Dec.	AOT	Target name	Result
2	316.757	+42.236	IRCZ4,a;Ns	NGC7027 (C)	Duplication (2)

# ID	R.A.	Dec.	AOT	Target name	d(') status
# 4081016	316.757	+42.236	IRC04,b;Ns	NGC7027 (CERN1,B)	0.0 Observed
# 1740550	316.757	+42.236	IRCZ4,b;Np	NGC 7027 (AGBGA,B)	0.0 Scheduled

ID	R.A.	Dec.	AOT	Target name	Result
3	84.088	-67.304	IRCZ4,b;Nh	SMP83 (B)	Duplication (1)

# ID	R.A.	Dec.	AOT	Target name	d(') status
# 1740328	84.087	-67.302	IRCZ4,b;Np	LMC-SMP083 (AGBGA,A)	0.1 Scheduled

ID	R.A.	Dec.	AOT	Target name	Result
4	84.088	-67.304	IRCZ4,a;Ns	SMP83 (C)	Duplication (1)

# ID	R.A.	Dec.	AOT	Target name	d(') status
# 1740328	84.087	-67.302	IRCZ4,b;Np	LMC-SMP083 (AGBGA,A)	0.1 Scheduled

Command executed on 2008/05/16_19:48:05 (JST).

Figure 1.3.11: Results from the Duplication Checker Tool. We see that our targets are in conflict with guaranteed time on AKARI and a previous OT observation in Phase 2. Duplication can be made on position, instrument/AOT and the number of pointings.

A.4 Example 3: Near-infrared imaging of extragalactic fields with the IRC

In this worked example we consider a program to image several deep extragalactic fields with the AKARI IRC-NIR instrument. We will simulate the preparation of the proposal from scientific background to proposal submission.

A.4.1 Scientific Background

Studies with the Infrared Space Observatory (ISO), of the Hubble Deep Fields have revealed star formation rates at least comparable to, or higher than those of optical/UV studies (Mann et al. 2002). At submillimetre wavelengths, surveys with SCUBA on the JCMT have revealed a large (>3000 deg^{-2} at $S850 > 2$ mJy) strongly evolving population of sources with bolometric luminosities $> 10^{12}$ L$_o$ and star formation rates of $\sim$ 300–1000 M$_\odot$ yr^{-1} with a median redshift of 2.4 (Chapman et al. 2003). The star formation rate at z$\sim$1 requires significant evolution in the IR galaxy population from the current epoch. Deep observations with the Spitzer Space Telescope have confirmed this strong evolution in the galaxy population out to ISO redshifts and furthermore provided insight into the higher redshift Universe in the so called redshift desert z$\sim$ 1–3 (Papovich et al. 2004). To connect the local and intermediate redshift IRAS/ISO Universe to the higher and high z Universe observed by Spitzer and SCUBA, comprehensive multiwavelength imaging is required throughout the extragalactic populations. Observations have been during Phase I and Phase II of the AKARI mission with the IRC-MIR-S & MIR-L cameras which have observed the full mid-infrared wavelength range in 6 bands from 7–24 μm to much higher sensitivities than obtained in the previous ISO surveys (Elbaz et al 2002) in order to constrain the dusty mid-infrared spectra of these sources.

Our targets are the same sources but at shorter wavelengths. Just as the mid-infrared observations can constrain the star-formation history of the Universe, the shorter near-infared wavelength bands can constrain the mass assembly history through the observation of the older stellar populations of these sources. It is known the stellar mass correlates well with the central black hole mass in massive galaxies (Magorrian et al. 1998) and by combining the near-infrared observations in Phase 3 with the previous results in Phase I & II we may move some way to constraining the energy budget of the Universe into the contributions from star-formation and black hole accretion.

For our program we will chose a set of well known fields where there is already a lot of follow up data including the Phase I and II observations with AKARI. These are the ISO-MARANO field, UKIDSS-UDS field, the COSMOS field, the HDF-N field, and the ISO southern ELAIS field. These fields are summarized in Table 1.4.6.

Table 1.4.6: Extragalactic target fields for observations with AKARI

Name	Equinox	R.A.	Dec.
ISO MARANO	J 2000	03:11:00.0	−54:45:00.0
UKIDSS-UDS	J 2000	02:21:20.0	−04:30:00.0
COSMOS	J 2000	10:00:28.60	+02:12:21.01
HDF-N	J 2000	12:36:49.9	+62:12:58.0
ELAIS-S1	J 2000	00:38:30.0	-44:00:00.0

A.4.2 Selection of Target Field and Target Visibility

A Visibility Tool is provided that gives an approximate estimation of the open time visibility of the target field during the Phase 3 of the AKARI mission. The available allocation for Open Time observations corresponds to around 6 pointings every day or almost a degree interval on the ecliptic longitude. Visibility is a strong function of ecliptic latitude and observations requiring very deep imaging and/or wide area mapping should choose their fields very carefully to avoid disappointment. Targets are input into the Visibility Tool in the same manner as described in the earlier sections. The results of the Visibility Tool for our fields are shown in Figure 1.4.12, the columns have already been explained in the first example in the cookbook section. The constraint on visibility can again be clearly seen in the input target fields. The Marano field is at a moderate ecliptic latitude of +35 degrees above the ecliptic while the COSMOS & UDS fields is only 9 & 17 degrees below the ecliptic plane respectively and is thus heavily constrained (only a total of 8 & 7 pointings in Phase 3 !). Combined with the poor visibility, we also find the Moon in the COSMOS field and it is thus probably unlikely that we will be able to carry out all our desired pointings. Therefore, we shall drop the COSMOS and UDS fields and concentrate on the remaining three fields.

The output from the visibility tool should be saved as an ASCII file as it will need to be uploaded as part of the final submission process for our proposal.

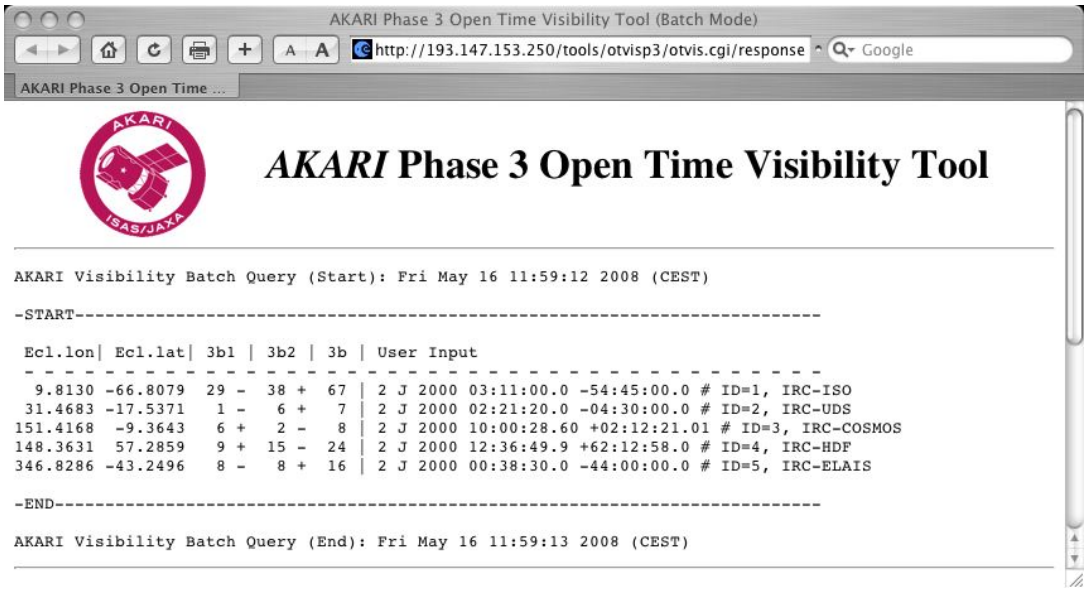

Figure 1.4.12: Results from the Visibility Tool in batch mode. The result shows the total number of allocations possible during Phase 3 of the AKARI mission. Each target is listed by position in Ecliptic coordinates, visibility in Phase 3b1 (2008 Oct. 15 – 2009 Apr. 11 = 179d), Phase 3b2 (2009 Apr. 12 – 2009 Oct. 14 = 186d) and the total visibility in Phase 3 (2008 Oct. 15 – 2009 Oct. 14 = 365d). The original user input is shown on the right.

A.4.3 The Choice of Observation Mode

The objective of the IRC observations is to detect the near-infrared emission from massive star-forming galaxies such as dusty ULIRGs. There are 3 observation AOTs available for near-infrared imaging.

1. AOT IRCZ0 : Formerly referred to as IRC00 or IRC05, this AOT carries out the deepest imaging in a single band only.

2. AOT IRCZ2 : Formerly referred to as IRC02, this AOT carries out intermediate depth imaging in two bands

3. AOT IRCZ3 : Formerly referred to as IRC03, this AOT carries out imaging in all three IRC bands (N2,N3,N4)

The typical flux densities for the colder ULIRGs in the near-infrared are around 10 μJy (see Figure 1.4.13). For our purpose, we require deep images of our fields, therefore we will select the IRCZ0 AOT. The current sensitivity estimates for this AOT are 18μJy in all three IRC bands which should be adequate to detect our sources (the multiband IRC AOT IRCZ3 has a sensitivity of around 40μJy which will probably be too shallow to detect our sources).

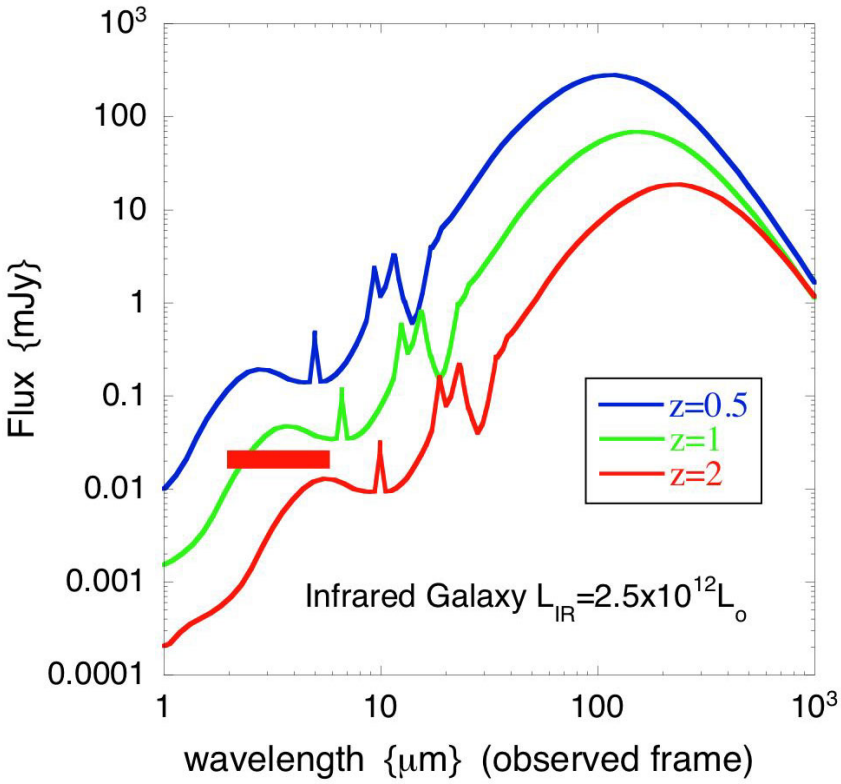

Figure 1.4.13: Estimated required sensitivities to detect dusty ULIRGs to redshift unity. We assume a single pointing with AOT IRCZ0.

A.4.4 Preparation of Target List

Once the AOTs have been selected we can go ahead and prepare the target list for our observations. An AKARI target list contains 1 line per target per AOT per field of view. We are observing our target fields with the IRC NIR camera using AOT IRCZ0, therefore we have 3 lines in our target list per target field (one each for the N2,N3 & N4 bands). We have 3 target fields, therefore we have a total of 9 lines in our target list. The target list is shown in Table 1.4.7. The target list consists of a unique I.D. in ascending but not necessarily contiguous

Table 1.4.7: Target List for submission

1, "IRC-ISO", "J2000", 03:11:00.0, -54:45:00.0, "IRCZ0", "b;N", 3, A, , "ISO FIRBACK"
2, "IRC-ISO", "J2000", 03:11:00.0, -54:45:00.0, "IRCZ0", "c;N", 3, B, , "ISO FIRBACK"
3, "IRC-ISO", "J2000", 03:11:00.0, -54:45:00.0, "IRCZ0", "a;N", 3, C, , "ISO FIRBACK"
4, "IRC-HDF", "J2000", 12:36:49.9, +62:12:58.0,"IRCZ0", "b;N", 3, A, , "HDF-N"
5, "IRC-HDF", "J2000", 12:36:49.9, +62:12:58.0,"IRCZ0", "c;N", 3, B, , "HDF-N"
6, "IRC-HDF", "J2000", 12:36:49.9, +62:12:58.0,"IRCZ0", "a;N", 3, C, , "HDF-N"
7, "IRC-ELAIS", "J2000", 00:38:30.0, -44:00:00.0,"IRCZ0", "b;N", 3, A, , "ELAIS-S"
8, "IRC-ELAIS", "J2000", 00:38:30.0, -44:00:00.0, "IRCZ0", "c;N", 3, B, , "ELAIS-S"
9, "IRC-ELAIS", "J2000", 00:38:30.0, -44:00:00.0, "IRCZ0", "a;N", 3, C, , "ELAIS-S"

order, followed by some identifier for the target name which should if possible be a resolvable by systems such as SIMBAD, NED. The next 3 fields are reserved for the coordinate system and target coordinates.

Following the AOT are the specific parameters for each given AOT. For the IRC imaging, we have to specify 2 parameters, the filter combination and the camera with which we want to observe. For the IRCZ0 AOT the filter can be chosen from parameters *a*,*b* or *c* (N2,N3 & N4 respectively). We require one target list line for each. The second parameter can only be *N* corresponding to the IRC-NIR camera.

In the following field we input the number of pointings for each AOT, for our case this has to be at least 3 for each IRCZ0 AOT. The reason for this is that this particular AOT (like the spectroscopic IRCZ4 AOT) is not dithered and the dithering has to be carried out be using different pointings. The observers themselves need do nothing since this operation will be carried out by the mission controllers.

We then have to prioritize our targets. AKARI Open Time Observations are divided into 3 priorities, *A* , *B*, *C* . Our *A* & *B* targets, barring any unforeseen events, should be observed, while the priority *C* targets should be considered as back-ups. In our target list, the number of priority *A* , *B*, *C* targets should be around the same. The objective of the IRC observations is to detect the near-infrared emission from massive star-forming galaxies to $z \sim 1$). Although multi-band detections are preferred the priority is a detection in at least one band. Therefore, for our observations we prioritize by IRC filter although we could just as easily prioritize by the observation field instead for example. We select the IRC N3 and N4 bands as priority *A* , *B* respectively. The N2 band is prioritized as C since in fact it is possible to make observations from the ground at this wavelength ($\sim 2\mu$m).

Finally, any notes are appended on the end of each target list line. Our final target list is shown in Table 1.4.7.

A.4.5 Target List Validation

The Target List syntax is validated in an identical manner to the previous imaging example. The target list will also be automatically validated when we upload it during the final proposal submission stage so there is no need for us to save the output of the Validation Check Tool at this stage.

A.4.6 Duplication Check Tool

Duplicate observations are decided on a basis of position, instrument/AOT and the number of pointings. This tool returns all IRC observations within a radius of 5 arcmins from the requested targets, which are either executed in the cold phase (Phase 1 and 2), or are in the blocked target list for Phase 3. Putting our target list into the Duplication Check Tool and selecting summary for the out put, we find that indeed there is a conflict of position or instrument for all of our observations in the HDF field (see Figure 1.4.14), and the TAC will have to look into the scientific justification to decide whether our observation is unique.

The output from the Duplication Check tool should be saved as an ASCII file as it will need to be uploaded as part of the final submission process for our proposal.

Query : target list: S=0, A=9, B=9, C=9, D=0 (total=27), search radius = 5.000 arcmin.

3 targets in your list are duplicated with the blocked target list.

ID	R.A.	Dec.	AOT	Target name	Result
1	47.750	-54.750	IRCZ0,b;N	IRC-ISO (A)	OK
2	47.750	-54.750	IRCZ0,c;N	IRC-ISO (B)	OK
3	47.750	-54.750	IRCZ0,a;N	IRC-ISO (C)	OK
4	189.208	+62.216	IRCZ0,b;N	IRC-HDF (A)	Duplication (8)

# ID	R.A.	Dec.	AOT	Target name	d(') status
# 1320028	189.208	+62.216	IRC05,c;N	GOODS-N-11 (FUHYU,A)	0.0 Observed
# 1320029	189.208	+62.216	IRC05,c;N	GOODS-N-11 (FUHYU,A)	0.0 Observed
# 1320030	189.208	+62.216	IRC05,c;N	GOODS-N-11 (FUHYU,A)	0.0 Observed
# 1320031	189.208	+62.216	IRC05,c;N	GOODS-N-11 (FUHYU,A)	0.0 Observed
# 1320032	189.208	+62.216	IRC05,c;N	GOODS-N-11 (FUHYU,A)	0.0 Observed
# 1320033	189.208	+62.216	IRC05,c;N	GOODS-N-11 (FUHYU,B)	0.0 Observed

5	189.208	+62.216	IRCZ0,c;N	IRC-HDF (B)	Duplication (8)

# ID	R.A.	Dec.	AOT	Target name	d(') status
# 1320028	189.208	+62.216	IRC05,c;N	GOODS-N-11 (FUHYU,A)	0.0 Observed
# 1320029	189.208	+62.216	IRC05,c;N	GOODS-N-11 (FUHYU,A)	0.0 Observed
# 1320030	189.208	+62.216	IRC05,c;N	GOODS-N-11 (FUHYU,A)	0.0 Observed
# 1320031	189.208	+62.216	IRC05,c;N	GOODS-N-11 (FUHYU,A)	0.0 Observed
# 1320032	189.208	+62.216	IRC05,c;N	GOODS-N-11 (FUHYU,A)	0.0 Observed
# 1320033	189.208	+62.216	IRC05,c;N	GOODS-N-11 (FUHYU,B)	0.0 Observed

6	189.208	+62.216	IRCZ0,a;N	IRC-HDF (C)	Duplication (8)

# ID	R.A.	Dec.	AOT	Target name	d(') status
# 1320028	189.208	+62.216	IRC05,c;N	GOODS-N-11 (FUHYU,A)	0.0 Observed
# 1320029	189.208	+62.216	IRC05,c;N	GOODS-N-11 (FUHYU,A)	0.0 Observed
# 1320030	189.208	+62.216	IRC05,c;N	GOODS-N-11 (FUHYU,A)	0.0 Observed
# 1320031	189.208	+62.216	IRC05,c;N	GOODS-N-11 (FUHYU,A)	0.0 Observed
# 1320032	189.208	+62.216	IRC05,c;N	GOODS-N-11 (FUHYU,A)	0.0 Observed
# 1320033	189.208	+62.216	IRC05,c;N	GOODS-N-11 (FUHYU,B)	0.0 Observed

7	9.625	-44.000	IRCZ0,b;N	IRC-ELAIS (A)	OK
8	9.625	-44.000	IRCZ0,c;N	IRC-ELAIS (B)	OK
9	9.625	-44.000	IRCZ0,a;N	IRC-ELAIS (C)	OK

Command executed on 2008/05/16_22:15:47 (JST).

Figure 1.4.14: Results from the Duplication Checker Tool. We see that 3 of our observations are in conflict with the guaranteed time on AKARI.

A.4.7 Submission of Proposal

After the duplication check, we can finally submit our proposal via the web interface. The proposal submission has several stages and we will need to upload various output files saved from the tools we used earlier. Each proposal has a 5 character abbreviation which will be used to identify each proposal. The next step is to upload the Target List which will be automatically verified (syntax only) on uploading. Following this we will be required to upload the results we saved from the output of the Visibility Tool, Duplication Check Tool and Instrument Performance Tool respectively. Once all these files have been uploaded we will have to enter the specific proposal information (name, address, telephone number, etc.) and general proposal information (Co-Is, category, title, abstract). The Scientific Justification must be submitted in PDF format and should not exceed 6 pages in total including scientific rationale, objective, references, figures and tables, and technical feasibility of the proposal. A confirmation page of the submission is created automatically. Shortly after, users will receive a formal confirmation by e-mail with the cover page of their proposal.